Aus dem Center for Stroke Research
der Medizinischen Fakultät Charité – Universitätsmedizin Berlin

DISSERTATION

Functional Neuroanatomy of Cerebello-Cerebral Systems

zur Erlangung des akademischen Grades
Doctor rerum medicinalium (Dr. rer. medic.)

vorgelegt der Medizinischen Fakultät
Charité – Universitätsmedizin Berlin

von

Judy A. Kipping, B.A., M.Sc

aus Berlin

Datum der Promotion: ......30.05.2015..............

Inhaltsverzeichnis

Abstrakt

Gegenstand derzeitiger neurowissenschaftlicher Forschung ist eine Zuordnung von Teilfunktionen zu räumlich definierten Hirnarealen innerhalb übergeordneter funktioneller Netzwerke. Während für das Großhirn eine Einteilung in zytoarchitektonisch definierte Gebiete eine gewisse funktionell-anatomische Basis vorgibt, ist die Kartierung funktioneller Teilbereiche im Kleinhirn erschwert durch seine einheitliche zytoarchitektonische Organisation. Statt histologischer Untersuchungen wurden Kleinhirnfunktionen im Menschen bisher vor allem durch klinische Läsionsstudien und Aktivierungs-Untersuchungen mittels funktioneller Bildgebung lokalisiert. Die Aussagekraft solcher Befunde ist jedoch durch die große interpersonelle Heterogenität sowie die Interpretationsschwierigkeiten angesichts unspezifischer Koaktivierungen bei funktioneller Bildgebung erheblich eingeschränkt. Ein vielversprechender Ansatz ist, die funktionelle Rolle von Kleinhirnarealen anhand ihrer Konnektivität zu spezifischen Großhirnstrukturen zu beschreiben. In invasiven tierexperimentellen Studien konnten mittels Tracer-Injektionen bereits Kleinhirnunterteilungen durch polysynaptische Verbindungen zu bestimmten Großhirnregionen identifiziert werden.

In der vorliegenden Arbeit wird dieser Ansatz – die funktionelle Kartierung von Subarealen des Kleinhirns anhand ihrer Konnektivität – auf nichtinvasive Untersuchungen am Menschen übertragen. Die Synchronisation von niederfrequenten Signalen im Gehirn, gemessen durch funktionelle Bildgebung, wird als funktionelle Konnektivität bezeichnet. Häufig untersuchte und replizierte Ergebnisse aus Tiermodellen und humanen Bildgebungsstudien lassen auf eine Gruppe von Kleinhirnlobuli (I-IV, V, VI, VIIIa/b) schließen, welche dem sensomotorischen System zugeordnet werden. Anhand dieser Kleinhirnregionen untersuchten wir, inwiefern basierend auf deren Konnektivitätsmustern bekannte und weniger erforschte funktionelle Teilbereiche im Kleinhirn beschrieben werden können.

Die vorliegende Arbeit umfasst drei Teile: (1) Qualitätseinschätzung der Kleinhirnsignale, (2) Kleinhirn-gesteuerte Konnektivitätskarten, (3) sublobulare Topographie des Kleinhirns.

Wir entwickelten einen Algorithmus, der durch Differenzierung von Kleinhirn- und Großhirnsignalen die Signalqualität in anatomisch beschriebenen Kleinhirnlobuli erheblich verbesserte. Mittels einer Korrelationsanalyse zwischen den gemittelten Zeitverläufen der aufgearbeiteten Kleinhirnlobuli und Großhirnsignalen konnten fünf kleinhirn-gesteuerte Netzwerke identifiziert werden. Die Großhirnregionen in diesen Netzwerken sind nicht nur assoziiert mit sensomotorischen Vorgängen, sondern auch bei affektiver und kognitiver Kontrolle, Sprache und Exekutivfunktionen involviert. Eine partielle Korrelationsanalyse der gemittelten Zeitverläufe aller beschriebenen Großhirnareale mit voxelbasierten Kleinhirnsignalen ermöglichte eine systematische Kartierung der Großhirnkonnektivität im Kleinhirn. Diese sublobulare Topographie indizierte parallele Netzwerke repräsentiert durch eine funktionelle Unterteilung innerhalb einzelner Lobuli. Jedoch wurden auch überlappende Konnektivitäten in den Lobuli gefunden.

Zusammengefasst belegt diese Arbeit für sensomotorisch bezogene Regionen, dass eine funktionelle Unterteilung anatomischer Kleinhirnlobuli mit nichtinvasiven Verfahren möglich ist. Zudem bietet sie eine neue Methode zur Verbesserung der Extrahierung relevanter Signale aus anatomisch unterteilten Hirnregionen. Basierend auf dieser Studie kann im nächsten Schritt eine konnektivitätsbasierte funktionell-anatomische Parzellierung des gesamten Kleinhirns vorgenommen werden. Damit sollte unser Verständnis über die funktionelle Organisation des Kleinhirns aber auch die funktionelle Lokalisierung von Kleinhirnschädigungen erheblich verbessert werden.

Abstrakt (Englisch)

The classification of subfunctions of spatially defined brain regions within large-scale functional networks is an important matter of neuroscientific research. Although cytoarchitectonic measures can be applied to the neocortex to map functional-anatomical subregions, the cerebellar cortex is a challenge due to its uniform cytoarchitecture. Instead of histological approaches, localized cerebellar functions have been inferred using clinical lesion studies and brain activation studies. However, the significance of their findings is limited by a large inter-subject heterogeneity and the difficulty of interpreting unspecific coactivation. A promising approach is to understand the role of the cerebellum in brain function by mapping its relationship to the rest of the brain. Invasive animal studies using tracing methods already provided cerebellar subdivisions through polysynaptic cerebello-cerebral connectivity.

In the current work, connectivity was measured using functional magnetic resonance imaging in humans, acquired during the resting-state. The synchronization of low-frequency fluctuations described by this data is used to characterize functional connectivity. Based on the well-studied primate sensorimotor system as well as human sensorimotor-related activation studies five cerebellar regions were selected (lobule I-IV, V, VI, VIIIa/b). By means of their connectivity patterns to the cerebrum, we investigated whether known and less well studied functional subdivisions could be described within and across these lobules.

The dissertation consists of three parts: (i) cerebellar signal assessment (ii) cerebello-driven connectivity maps, (iii) cerebellar sublobular topography.

We developed an algorithm which substantially improved the signal-to-noise ratio in anatomically defined cerebellar lobules by differentiating cerebellar and cerebral signals. In a correlation analysis, the mean time series of the refined cerebellar lobules revealed five cerebello-driven brain networks. The regions in those cerebral networks have been found to not only process sensorimotor information, but to also be involved in affective and cognitive control, language and executive functions. A subsequent partial correlation analysis of the mean cerebral time series with voxelwise cerebellar time series provided a systematic mapping of cerebral

connectivity in cerebellar lobules. This functional sublobular topography indicated parallel networks, though also overlapping connectivity was found within and across lobules.

In conclusion, this thesis provides – in respect to sensorimotor-related regions – the basis for functional subdivisions within anatomical cerebellar lobules using noninvasive imaging. Additionally, it introduces a method to improve extraction of relevant signal from anatomically delineated regions. Based on these results, a connectivity-based parcellation of the entire cerebellum has the potential to substantially expand our understanding of cerebellar functional organization, and enable functional localization of cerebellar damages.

Eidesstattliche Versicherung

„Ich, Judy Kipping, versichere an Eides statt durch meine eigenhändige Unterschrift, dass ich die vorgelegte Dissertation mit dem Thema: Functional Neuroanatomy of Cerebello-Cerebral Systems selbstständig und ohne nicht offengelegte Hilfe Dritter verfasst und keine anderen als die angegebenen Quellen und Hilfsmittel genutzt habe.

Alle Stellen, die wörtlich oder dem Sinne nach auf Publikationen oder Vorträgen anderer Autoren beruhen, sind als solche in korrekter Zitierung (siehe „Uniform Requirements for Manuscripts (URM)" des ICMJE -*www.icmje.org*) kenntlich gemacht. Die Abschnitte zu Methodik (insbesondere praktische Arbeiten, Laborbestimmungen, statistische Aufarbeitung) und Resultaten (insbesondere Abbildungen, Graphiken und Tabellen) entsprechen den URM (s.o) und werden von mir verantwortet.

Meine Anteile an den ausgewählten Publikationen entsprechen denen, die in der untenstehenden gemeinsamen Erklärung mit dem/der Betreuer/in, angegeben sind. Sämtliche Publikationen, die aus dieser Dissertation hervorgegangen sind und bei denen ich Autor bin, entsprechen den URM (s.o) und werden von mir verantwortet.

Die Bedeutung dieser eidesstattlichen Versicherung und die strafrechtlichen Folgen einer unwahren eidesstattlichen Versicherung (§156,161 des Strafgesetzbuches) sind mir bekannt und bewusst."

_____

Datum   24.03.2014   Unterschrift

Anteilserklärung an der erfolgten Publikation

Judy Kipping hatte folgenden Anteil an der folgenden Publikation:

Autoren: Judy A. Kipping, Wolfgang Grodd, Vinod Kumar, Marco Taubert, Arno Villringer, Daniel S. Margulies

Titel: Overlapping and parallel cerebello-cerebral networks contributing to sensorimotor control: An intrinsic functional connectivity study

Zeitschrift: NeuroImage

Erscheinungsjahr: 2013

Beiträge im Einzelnen:

90 % Konzeptentwicklung

95 % Entwicklung der beschriebenen methodischen Analyse

90 % Datenanalyse und statistische Auswertung der Ergebnisse

90 % Verfassung der Publikation

90 % Bearbeitung und Korrekturen im Reviewverfahren

Unterschrift, Datum und Stempel des betreuenden Hochschullehrers/der betreuenden Hochschullehrerin

_____

Unterschrift des Doktoranden/der Doktorandin

_____

Auszug aus der Journal Summary List

ISI Web of Knowledge℠

Journal Citation Reports®

WELCOME　　HELP

VIEW CATEGORY SUMMARY LIST

Impact Factor　　SORT AGAIN

MARK ALL　　UPDATE MARKED LIST

Ranking is based on your journal and sort selections.

		(linked to journal information)									Eigenfactor ⓘ	
											Eigenfactor	Article Influence
☐	21	J PINEAL RES	0742-3098	4956	7.304	5.451	1.109	92	5.2		0.00734	0.842
☐	22	J NEUROSCI	0270-6474	160915	6.908	7.869	0.978	1668	7.5		0.43823	3.170
☐	23	HUM BRAIN MAPP	1065-9471	13379	6.878	7.032	1.451	226	5.9		0.04165	2.592
☐	24	CEREB CORTEX	1047-3211	21409	6.828	7.463	2.050	258	6.0		0.07485	3.117
☐	25	NEUROPSYCHOL REV	1040-7308	1611	6.420	7.526	0.862	29	5.1		0.00631	2.717
☐	26	NEUROIMAGE	1053-8119	61770	6.252	7.063	1.291	1222	6.0		0.16507	2.285
☐	27	J PSYCHIATR NEUROSCI	1180-4882	2253	6.242	6.473	1.647	34	5.2		0.00690	2.148
☐	28	NEUROBIOL AGING	0197-4580	15479	6.166	6.098	1.583	537	6.1		0.03535	1.837
☐	29	CORTEX	0010-9452	5265	6.161	5.042	2.745	106	5.3		0.01386	1.575
☐	30	NEUROTHERAPEUTICS	1933-7213	1923	5.904	5.720	0.905	63	3.6		0.01022	1.817
☐	31	PAIN	0304-3959	29370	5.644	6.125	1.264	269	9.0		0.04797	1.855
☐	32	INT J NEUROPSYCHOPH	1461-1457	4003	5.641	5.092	0.805	123	3.9		0.01365	1.475
☐	33	NEUROSCIENTIST	1073-8584	3259	5.633	6.417	1.356	45	6.1		0.00990	2.363
☐	34	NEUROBIOL DIS	0969-9961	11288	5.624	5.482	1.493	296	5.1		0.03352	1.727
☐	35	BRAIN BEHAV IMMUN	0889-1591	6137	5.612	5.698	1.082	147	4.3		0.02194	1.719
☐	36	HIPPOCAMPUS	1050-9631	8046	5.492	5.484	1.603	184	6.7		0.02126	2.081
☐	37	MOL NEUROBIOL	0893-7648	2715	5.471	5.535	0.782	101	5.7		0.00753	1.789
☐	38	CURR OPIN NEUROL	1350-7540	4449	5.416	5.035	0.804	97	5.6		0.01391	1.742
☐	39	J CEREBR BLOOD F MET	0271-678X	14671	5.398	5.660	1.093	194	8.0		0.03150	1.867
☐	40	FRONT AGING NEUROSCI	1663-4365	392	5.224	5.169	0.727	33	2.4		0.00198	1.597

MARK ALL　　UPDATE MARKED LIST

THOMSON REUTERS

Published by Thomson Reuters

Der Dissertation zugrundeliegende wissenschaftliche Publikation
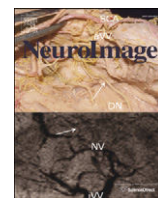
Overlapping and parallel cerebello-cerebral networks contributing to sensorimotor control: An intrinsic functional connectivity study

Judy A. Kipping [a], Wolfgang Grodd [e], Vinod Kumar [e], Marco Taubert [a], Arno Villringer [a,c,d], Daniel S. Margulies [b,*]

[a] Department of Neurology, Max Planck Institute for Human Cognitive and Brain Sciences, Stephanstrasse 1a, 04103 Leipzig, Germany
[b] Max Planck Research Group: Neuroanatomy & Connectivity, Max Planck Institute for Human Cognitive and Brain Sciences, Stephanstrasse 1a, D-04103 Leipzig, Germany
[c] Center for Stroke Research Berlin, Charité–Universitätsmedizin Berlin, Charitéplatz 1, 10117 Berlin, Germany
[d] Berlin School of Mind and Brain, Humboldt University, Luisenstrasse 56, 10117 Berlin, Germany
[e] Psychotherapy and Psychosomatics, University Hospital Aachen, Department of Psychiatry, Pauwelsstraße 30, 52074 Aachen, Germany

ARTICLE INFO

ABSTRACT

In concert with sensorimotor control areas of the cerebrum, the cerebellum shows differential activation patterns during a variety of sensorimotor-related tasks. However, the spatial details and extent of the complex and heterogeneous cerebello-cerebral systems involved in action control remain uncertain. In this study, we use intrinsic functional connectivity (iFC) to examine cerebello-cerebral networks of five cerebellar lobules (I–IV, V, VI, and VIIIa/b) that have been empirically identified to form the functional basis of sensorimotor processes. A refined cerebellar seed-region selection allowed us to identify a network of primary sensorimotor and supplementary motor areas (I–V), a network of prefrontal, premotor, occipito-temporal and inferior-parietal regions (VI), and two largely overlapping networks involving premotor and superior parietal regions, the temporo-parietal junction as well as occipito-temporal regions (VIIIa/b). All networks involved the medial prefrontal/cingulate cortex. These cerebral clusters were used in a partial correlation analysis to systematically map cerebral connectivity throughout the entire cerebellum. We discuss these findings in the framework of affective and cognitive control, sensorimotor, multisensory systems, and executive/language systems. Within the cerebellum we found that cerebro-cerebellar systems seem to run in parallel, as indicated by distinct sublobular functional topography of prefrontal, parietal, sensorimotor, cingulate, and occipito-temporal regions. However, all areas showed overlapping connectivity to various degrees in both hemispheres. The results of both analyses demonstrate that different sublobular parts of the cerebellar lobules may dominate in different aspects of primary or higher-order sensorimotor processing. This systems-level cerebellar organization provides a more detailed structure for cerebello-cerebral interaction which contributes to our understanding of complex motor behavior.

© 2013 Elsevier Inc. All rights reserved.

Introduction

Throughout the evolution of mammals, the cerebellum and the cerebral cortex have evolved in parallel. Their respective sizes have proportionally increased, and the connections between both have also substantially grown during phylogeny (Sultan, 2002; Sultan and Glickstein, 2007). The first combined cerebellar-cerebral function was coordination of movement involving both motor planning and execution (Holmes, 1939; Thach, 1997). In humans and great apes, the demands for sensory discrimination, sensorimotor integration and motor coordination have increased, requiring additional cerebellar contributions (Manto et al., 2012). The cerebellum contributes to diverse functions such as flexible motor action, execution of complex movements and successful learning of new movement strategies (Smaers et al., 2011; Stein and Glickstein, 1992; Thach, 1998). One cerebellar role is to provide predictive values about the outcome of an intended goal, which allows for the preparation of neural systems in the cerebrum that are likely to be responsive to the task at hand (Courchesne and Allen, 1997). Both the estimated prediction of outcomes as well as the preparation of neural systems enable cost-optimal and goal-accomplishing movements.

In this study we specifically focused on widespread cerebral connectivity, which has been investigated in the primate brain using transsynaptic tract-tracing studies in the macaque monkey (Kelly and Strick, 2003; Lu et al., 2007; Middleton and Strick, 2000; Orioli and Strick, 1989). It has been demonstrated that the cerebellar output is composed of a number of separate but parallel "output channels" (Middleton and Strick, 1997). The underlying anatomical relationship of the sensorimotor system mainly comprises afferent connections of cerebellar lobules III–VI and VIIb–VIII via the deep cerebellar nuclei to the midbrain and thalamus, and subsequently to premotor and motor

cortex. Efferent connections project back via the pontine nuclei to lobules V–VI and VIIb–VIII in a closed-loop fashion (Kelly and Strick, 2003).

Anatomical connections established in the macaque monkey have been indirectly validated in humans by corresponding activation patterns in imaging studies using positron emission tomography and functional magnetic resonance imaging (fMRI). fMRI movement paradigms in humans, which involve simple and natural muscular flexion and extension, have revealed movement-related cerebellar representations which mapped foot, tongue and hand, which are restricted to the lobules IV, V, VI and VIII (Grodd et al., 2001; Rijntjes et al., 1999).

Lobules IV and V are consistently activated during the planning and execution of simple movements of body parts (Grodd et al., 2001; Schlerf et al., 2010). With respect to lower-level motor functions these areas appear to have somatotopic organization, which is similar in monkeys and cats (Snider and Eldred, 1952), as well as in humans (Grodd et al., 2001). However, in addition to the movement-related cerebral inputs, lobule V also receives proprioceptive information from spinal inputs, whose signals both converge on the same Purkinje cells as shown in cats (Allen et al., 1974). Consequently, lobule V has been found to be activated during passive and active movements (Jueptner et al., 1997; Thickbroom et al., 2003; Wiestler et al., 2011), tactile stimulation (Wiestler et al., 2011) and in the prediction of the sensory consequences of a movement (Blakemore et al., 1998), indicating an involvement in sensory as well as motor processes.

With increasing complexity of coordinated movements as evoked by higher rates of tapping (Jancke et al., 1999) or sequential movements (Schlerf et al., 2010), parts of lobule VI have been shown to accompany the motor-evoked activation in lobule V and more anterior lobules using fMRI in humans. Lobule VI has also been found to be specifically activated during the storage of acquired kinematic tool use (Imamizu et al., 2000). An index finger movement task with self-paced delay showed a temporal dissociation in sensorimotor processing (Hulsmann et al., 2003). Whereas lobule VI was recruited 3 s prior to movement onset, activation in lobule V followed close to and after movement onset. In contrast, Cui et al. (2000) report a lack of functional dissociation between preparation and execution of coordinated movements within bilateral lobules V–VII. These diverse fMRI results show that lobules IV, V, and VI may contribute to different phases of sensorimotor events.

Lobule VIII is activated during simple active and passive sensorimotor tasks, and therefore has been proposed to possess similar functions as lobule V, which is the representation of motor and sensory processes (Thickbroom et al., 2003). In both lobules, active performance as well as tactile stimulation reveal superimposed sensory and motor maps (Wiestler et al., 2011). However, despite this similarity, lobule VIII has been found to play a role in sensory feedback accompanying basic motor processing in lobule V (Habas and Cabanis, 2008) and in the timing of more complex and voluntary movements (Habas et al., 2004). Recent exploration of lobule VIII found a functional contribution of lobular segments VIIIa and VIIIb to finger tapping and verb generation (Stoodley et al., 2012).

The fMRI findings of overlapping cerebro-cerebellar networks involved in sensorimotor tasks complicate the functional assignments of cerebellar lobules IV, V, VI, and VIII. These cerebellar regions likely reveal differential involvement in domains involved in planning, execution, and control of movements and are thus engaged in various brain networks.

Evaluating human cerebello-cerebral connectivity using iFC

Three studies published in 2009 (Habas et al., 2009; Krienen and Buckner, 2009; O'Reilly et al., 2010) used iFC to depict major cerebro-cerebellar iFC networks within the sensorimotor as well as non-motor domains in humans. In addition to dedicated cortical areas, subcortical components—including the midbrain and thalamus (Middleton and

Strick, 1997; Sommer, 2003)—have been shown to participate in various iFC networks (Habas et al., 2009). The sensorimotor nature of cerebellar lobules V, VI, and VIII (and particularly VIIIb; according to a peak cerebellar coordinate in Krienen and Buckner (2009)) has been validated using iFC (Krienen and Buckner, 2009; O'Reilly et al., 2010). Buckner et al. (2011) recently demonstrated a further differentiation. They show that lobules IV and V are sensorimotor related, lobule VI is part of the sensorimotor, ventral attention and fronto-parietal network, and lobule VIII is part of the sensorimotor and the ventral attention network. Very recently, Sang et al. (2012) investigated the cerebellar connectivity of the hemispheres and vermis. They found that lobules I–VI are connected to the visual and sensorimotor network; lobule VI to the auditory, the salience and sensorimotor network; and lobule VIIIb to the salience, sensorimotor, task-positive and the default mode network. However, if the cerebellum is connected to various regions within the cerebrum, the question remains as to what extent these cerebellar regions have overlapping or distinct connectivity patterns. The study by Buckner et al. (2011) applied a winner-take-all algorithm, which separates regions based on their strongest connectivity to large-scale cerebral resting-state networks, but does not allow for overlapping connectivity patterns. In contrast, the study by Sang et al. (2012) used one-sample t-tests for each lobule, which does not account for common variance across adjacent lobules, potentially introducing false positive overlapping connectivity results. Even though they quantified the connectivity maps of lobules VII and VIII, the more anterior cerebellar lobules were not addressed. Due to the variable methodology, it remains unclear whether the cerebellar regions have overlapping or separate connectivity patterns.

We therefore extended the examination of cerebellar lobules by introducing a refined seed definition for seed-based iFC analysis which addresses the false positive connectivity to adjacent cerebral and non-brain tissue (see also Buckner et al. (2011)). This refinement consisted of removing all voxels which were contaminated by adjacent non-cerebellar tissue. To enhance our understanding of the separate and overlapping cerebello-thalamo-cerebral pathways, we first investigated connectivity of cerebellar lobules I–IV, V, VI, and VIIIa/b with large-scale cerebral networks. This cerebello-centric approach was then complemented by a voxelwise iFC analysis beginning in the cerebrum. We were thus able to systematically identify overlapping and parallel functional regions on a sublobular level. We interpret the cerebellar mapping in the context of their associated cerebral functional subsystems.

Material and methods

Participants

We included 38 MR data sets from healthy participants (25 female; mean age of 30.34 ± 7.51 years), distributed by the 1000 Functional Connectome Project (http://fcon_1000.projects.nitrc.org/indi/pro/Berlin.html). Two resting state scans were acquired during a single scanning session for each participant. Functional images were visually inspected to ensure that the ventral parts of the cerebellum (esp. lobule VIIIa/b) were acquired. Only those data sets that included the inferior portion of the cerebellum were included, thus restricting this study to 38 of 50 data sets.

Data acquisition

MR images were acquired at a 3 T Magnetom Tim Trio Siemens scanner using a 12 channel phased-array head coil. In each of the two resting state scanning sessions, 200 whole brain volumes were acquired including the entire cerebellum using echo-planar image (EPI) pulse sequences with 34 axial slices (TR = 2300 ms, TE = 30 ms, flip angle 90°, slice thickness = 4 mm, $3 \times 3 \times 4$ mm voxels, interleaved ascending slice acquisition, acquisition matrix = 64×64,

bandwidth = 2232 Hz, duration = ~7.5 min). During the resting state scan participants were instructed to remain relaxed while keeping their eyes open. A high-resolution T1-weighted scan was acquired with a MPRAGE (magnetization-prepared rapid acquisition gradient echo) sequence (TR = 2.3 s; TE = 2.98 ms; flip angle = 9°, FOV = 256; 176 sagittal slices; voxel size = $1 \times 1 \times 1$ mm) covering the whole brain for anatomical reference.

Data preprocessing

Image preprocessing of the resting state data was performed with FSL (Smith et al., 2004), AFNI (Cox, 1996), SPM8 (http://www.fil.ion. ucl.ac.uk/SPM, Welcome Department of Imaging Neuroscience, London, UK), and in-house scripts written in MatLab (http://www. mathworks.com, Cambridge, UK).

The main preprocessing steps are described here, and are also available in further detail in the scripts distributed by 1000 Functional Connectome Project (http://fcon_1000.projects.nitrc.org). The first four time points (9.2 s) of the two scanning sessions were discarded to reach equilibrium of magnetization. In SPM, the origins of functional and anatomical data were reoriented to the anterior commissure for within-subject registration. Anatomical images were realigned to reoriented functional images. Sequential slice acquisition during EPI acquisition was accounted for by shifting each slice in time to be aligned with the middle slice (FSL). Correction for small movement artifacts was performed by estimating the spatial deviations between the mean functional reference image and each functional image (AFNI). The frequency spectrum was band-pass filtered (0.01–0.1 Hz) to remove nuisance signals (AFNI). Drifts originating from the MR scanner were removed by linearly detrending the functional data. In order to remove signal from non-gray matter tissue, six motion parameters as well as signals from white matter (WM) and cerebro-spinal fluid (CSF) masks were removed using multiple regression (FSL). Masks of WM and CSF resulted from tissue segmentation (FSL), were inspected visually and modified such that only the tissue of interest was included. Global signal was not removed due to previous findings that global signal is also partially of neuronal origin (Scholvinck et al., 2010). Using SPM, anatomical data was segmented into gray matter, WM and CSF. By means of the transformation matrix from the segmentation step, functional images were brought into standard stereotactic Montreal Neurological Institute (MNI) space using spatial non-linear normalization (SPM) with a 2 mm³ voxel size. SPM normalization was used because we wished to take advantage of the cerebellar normalization provided with the SPM toolbox SUIT (see below). Before smoothing the cerebellum was masked to minimize the cross-structure signal contamination. Afterwards, a Gaussian kernel with 4 mm full-width half-maximum (FWHM) was applied separately to the cerebrum (FSL).

Cerebellar normalization

Diedrichsen (2006) developed a spatially unbiased atlas template of the cerebellum and brainstem (SUIT) and a cerebellum-only normalization (provided by SUIT) because whole-brain spatial normalization to MNI space can cause elongation along the cerebellar z-axis. Furthermore, the highly smoothed ICBM152 MNI template leaves the fine cerebellar folia almost invisible. Therefore, cerebella were separately normalized using the SPM toolbox SUIT, which is in the space defined by MNI152 template and uses the anatomical labels provided by the MRI atlas from Schmahmann et al. (1999). The segmentation of the cerebellum was visually inspected and hand-corrected to ensure the accuracy of the mask. A spatial non-linear normalization (same as used for cerebral normalization) to the SUIT template was performed utilizing the individual cerebellar masks. The preprocessed functional data were resliced using the deformation matrix of the anatomical normalization process and afterwards smoothed with a 4 mm FWHM Gaussian kernel.

Cerebellar ROI definition and cerebello-cerebral signal separation

The iFC analysis is based on the hypothesis that different cerebellar lobules are involved in action control. Due to a lack of sublobular parcellation, we have utilized anatomical masks of cerebellar lobules for a voxelwise seed-based correlation analysis. Even though we were interested in above mentioned ten anatomical lobules, all 20 anatomical lobular ROIs (aROIs) were chosen from the SUIT template (Diedrichsen et al., 2009) in order to account for common variance across adjacent lobules (Fig. 2B). Lobular binary masks are based on the maximum probability maps of the SUIT atlas (Diedrichsen et al., 2009). The signals within each aROI includes voxels that are contaminated by non-cerebellar signals from the surrounding tissue such as CSF or adjacent visual cortex. The following method aimed to remove such voxels from further analysis. In order to determine whether a voxel contained more cerebellar than cerebral signal, we took advantage of the high correlation between interhemispheric cerebral homologs (Stark et al., 2008). The following analysis was thus based on the assumption that pure cerebellar signals are more correlated across hemispheres than with adjacent cerebral signals. A higher correlation between time series of cerebellar homologs as compared to non-homologs provides support for a similar interhemispheric synchrony in the cerebellum as previously observed in the cerebrum (Stark et al., 2008). Supplementary Fig. 1 demonstrates the mean intracerebellar correlation.

20 anatomical cerebellar masks were functionally constrained by separating the voxels, whose time series correlated more with either a cerebellar or cerebral signal. The mean BOLD signal from the homotopic cerebellar region (Fig. 1, step 1b) was used as the "cerebellar signal" whereas the mean BOLD signals from ipsilateral adjacent cerebral areas (lingual gyrus, fusiform gyrus, parahippocampal gyrus, and lateral occipital gyrus) were utilized as "noise signals" (Fig. 1, step 1c): Let x_n be a voxel, where n is the index of a voxel in a cerebellar mask of interest (Fig. 1, step 1a and 2), y is the mean signal of the contralateral homolog (Fig. 1, step 3a). Then voxel x_c is a functionally relevant cerebellar voxel, if the correlation between x_n and y was stronger than between x_n and any of the mean signals of adjacent cerebral areas (Fig. 1, step 3b) using a winner-take-all algorithm (Fig. 1, step 4). For each of the two individual scans, two binary masks with voxels, which were either more strongly correlated to the "cerebellar" signal or to a "noise" signal, were created (Fig. 1, step 5). The intersection of the two "cerebellar" masks entered a group-level comparison. On the group-level, a probabilistic cerebellar map was created and arbitrarily thresholded at 85% (32 out of 38 subjects), i.e. those remaining "cerebellar" voxels were considered as functionally relevant within the anatomical mask (Fig. 1, step 6 and 7). After labeling the functionally relevant voxels according to the anatomical masks, the cerebello-cerebral separation process was iterated a second time (Fig. 1, repetition of steps 1a, 1c, 2–7). But instead of correlating cerebellar voxels' time series to a mean signal of the homotopic cerebellar lobule, the mean signals of the new set of functionally relevant cerebellar voxels' time series were taken as references (Fig. 1, step 8).

Seed-based correlation analysis

Within the anatomical masks (aROIs) only functionally-relevant cerebellar voxels were used to examine cerebello-cerebral iFC of cerebellar lobules I–IV, V, VI, and VIIIa/b (scheme in Fig. 2A, left). However, all 20 cerebellar fROIs were used as weights in the following ANOVA. Therefore, the mean time series of functionally relevant voxels within each of the 20 lobules (fROIs) were correlated with all voxels within the cerebrum (Fig. 1, steps 9 and 10). The resulting matrices of Pearson's product moment correlation coefficients were Fisher's *r*-to-*z* transformed (two per individual) and averaged within individuals for each of the 20 fROIs (Fig. 1, step 10). For the group-level, the *r*-to-*z* transformed maps of each lobule entered a one-way
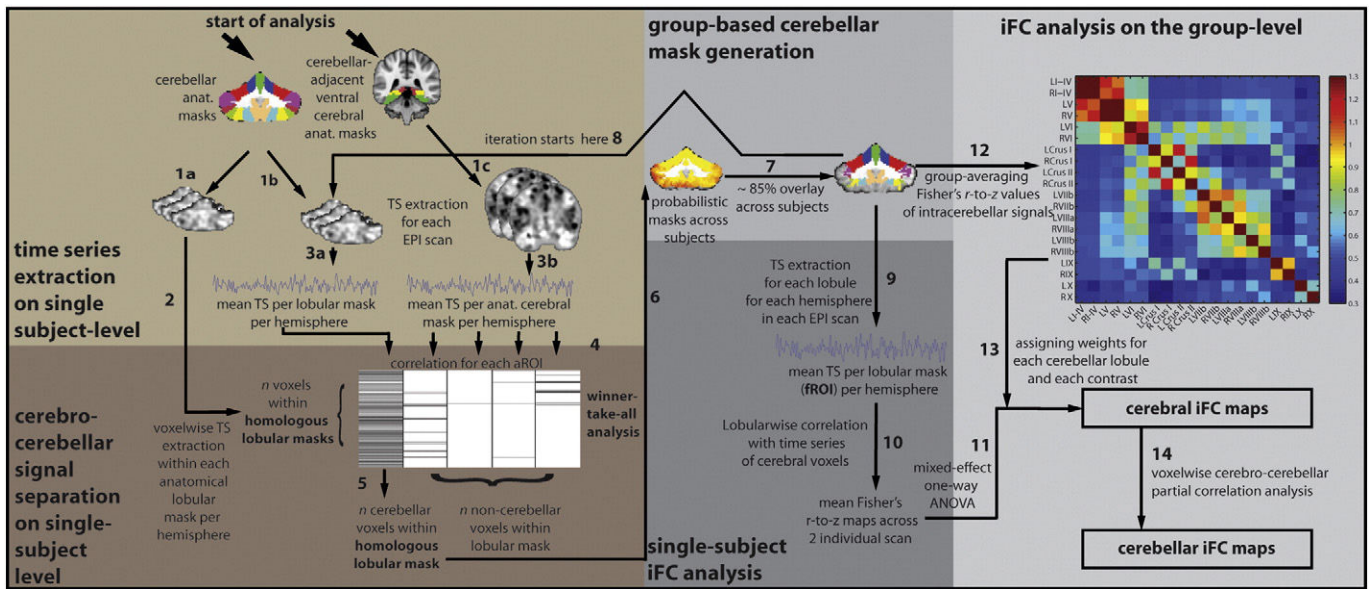
Fig. 1. Methods schematic for seed selection on the single-subject level (brown areas) and cerebral and cerebellar iFC map generation (gray areas). Numbers indicate the stepwise processes (see text). TS, time series; iFC, intrinsic functional connectivity.

mixed-effects ANOVA (analysis of variance) with 20 levels of a single factor, which represented the 20 lobules (Fig. 1, step 11). While this factor remained fixed, subjects were considered to be random. We investigated the fraction of the total variance that can be explained by each lobule. Therefore, each lobule was contrasted against all other lobules in a weighted-ANOVA. The contrast values for each lobule represented weights which indicated how strongly a mean lobular signal was correlated to the signals of the other lobules. Therefore, all 20 signals from the cerebellum were correlated within each individual. Pearson's product moment correlation coefficients were Fisher's r-to-z transformed and averaged across individuals (Fig. 1, step 12).

For the purpose of contrasting, r-to-z transformed values were set to a range between 0 and 1 by dividing each r-to-z value by the sum of r-to-z values (Fig. 1, step 13). A lobule of interest received value 1 and all others the negative of the normalized z-value. High correlations yielded a high contrast value and low correlation values a low contrast value. The same analysis was performed with aROIs (instead of fROIs). The r-to-z matrices using signals of fROIs and aROIs are displayed in Supplementary Fig. 1. All connectivity maps were multiplied with a subcortico-cortical Harvard-Oxford mask (Desikan et al., 2006) and corrected for multiple tests over the voxels within the gray-matter mask (p < 0.001, voxelwise FDR corrected).
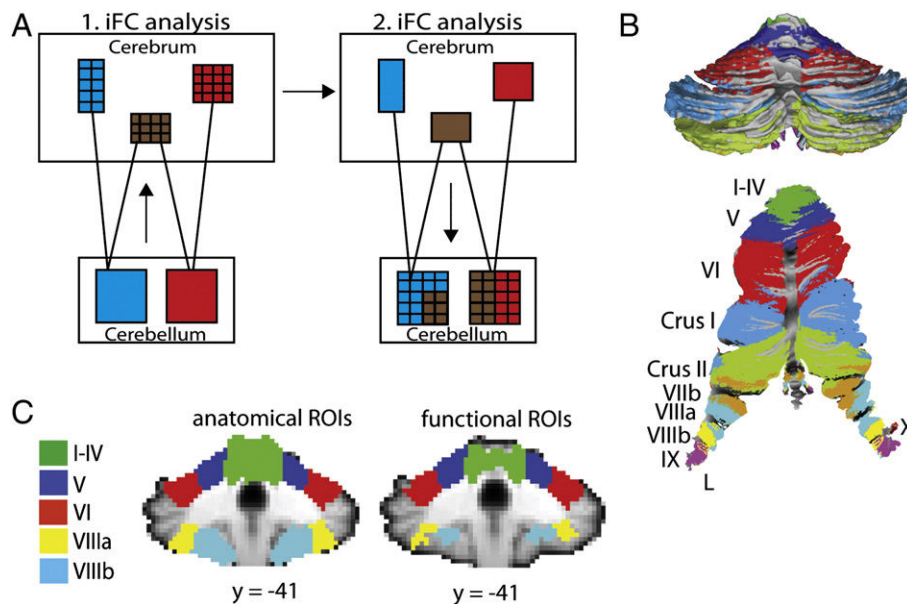

Fig. 2. (A) Analysis scheme of a voxelwise cerebello-cerebral analysis and a subsequent voxelwise cerebro-cerebellar analysis. The combination of both analyses aimed at revealing first subcomponents of large-scale cerebral networks, which are connected to different cerebellar lobules. Secondly, overlapping and unique connectivity of cerebral regions has been identified in the cerebellum. (B) Anatomical cerebellar masks on a partially inflated surface map (top) and on a cerebellar flat map (bottom) displayed for anatomical reference (Diedrichsen, 2006; Van Essen et al., 2001). (C) Anatomical masks (aROIs) and functional masks (fROIs) created by cerebello-cerebral signal separation are displayed on single coronal slices to show the reduction of voxels at cerebellar borders.

Cerebral connectivity within the cerebellum

The contrast analysis revealed connectivity patterns to cerebral areas. The subsequent analysis addressed whether and how the connectivity of cerebral areas is distributed within and across cerebellar anatomical borders (Fig. 1, step 14). For this, the cerebral clusters served as seed regions (scheme in Fig. 2A, right) and the analysis was performed for left and right cerebellar hemispheres separately. As a first step, cerebral clusters were eroded and dilated to receive the largest supra-threshold clusters and to remove bridges between clusters. The following criteria have been chosen for cluster selection. First, we restricted our analysis to cerebral regions that were found for both left and right cerebellar homologs. Second, for each cerebello-cerebral iFC map separately, we collapsed the signals of homologous cerebral clusters, if present. Each of the sets of cerebral clusters (as defined by the five cerebellar fROIs) was entered separately into a partial correlation analysis to reduce contributions from global and third-party effects to specific cerebro-cerebellar correlations (Hampson et al., 2002). For each of the two scans of each individual, the mean time series of cerebral clusters which were connected to the five left fROIs was correlated with cerebellar time series of all ten left fROIs. The same correlation analysis was performed for cerebral clusters connected to the right cerebellum. Pearson's correlation coefficients were Fisher's r-to-z transformed and averaged across the two individual scans. Voxelwise t-tests determined connectivity of each cerebral cluster at every cerebellar voxel, so that we could identify how the connectivity is distributed at the sublobular level, while allowing for separate or overlapping cerebral connectivity. To differentiate spatial patterns of those highly connected cerebellar and cerebral sets of regions, a more stringent threshold was required ($p < 0.00001$, voxelwise FDR corr.). At a more liberal threshold of $p < 0.001$ cerebral clusters showed substantial overlap, some of which occurred between regions as functionally separate as prefrontal and sensorimotor areas. For the purposes of visualization, we mapped cerebral cluster combinations in the cerebellar hemispheres, if a combination was present in at least five voxels (<0.1% of all hemispheric fROIs) in the corresponding cerebellar hemisphere.

Results

Optimized functional connectivity of cerebellar lobules

All cerebellar lobules in both hemispheres were targeted to undergo cerebello-cerebral signal separation. The number of voxels included in our five fROIs and aROIs (I–IV, V, VI, and VIIIa/b) are presented in Table 1, and the masks are presented in Fig. 2C. fROIs within lobules V and VI included ~90% of voxels from the anatomical masks and seemed to be the least contaminated. In lobules I–IV ~70%, in lobule VIIIa ~50%, and in lobule VIIIb ~30% of voxels survived the cerebello-cerebral separation. The voxels remaining in the fROIs, irrespective of the lobule, were distant from the cerebellar border as can be seen in Fig. 2C. Furthermore, the mean SNR values for every lobule increased with reduction in the number of "noise" voxels (Supplementary Fig. 2).

Delineating cerebello-cerebral subsystems

The results of this analysis represent the unique cerebello-thalamo-cerebral functional networks within the sensorimotor and associated higher-order sensorimotor systems. We found a sensorimotor network involving cerebellar lobules I–V. Lobule VI was connected to a higher-order executive network. Lobules VIIIa/b were part of a multisensory network. Lobules V, VI, and VIIIa/b were connected to various parts of the medial prefrontal/cingulate cortex, regions involved in affective and cognitive control.

Fig. 3 represents thresholded and color-coded cerebral and thalamic iFC patterns derived from the weighted-ANOVA using fROIs, where color labels indicate the corresponding cerebellar fROIs.

Table 1
Number of voxels in anatomical and functional ROIs. Volume sizes, center of mass co-ordinates, and location of cerebral areas, which showed iFC to the respective cerebellar fROIs are reported and represent areas that have been used for partial correlation analysis.

Lobule	Size of aROIs (voxels)	Size of fROIs (2nd run)	Size of cerebral clusters (voxels)	MNI coordinates (x, y, z)	Cerebral clusters
Left I–IV	630	427 (67.78%)	46	10, −22, 71	Right SM*
Right I–IV	662	404 (61.03%)	–	–	–
Left V	779	730 (93.71%)	2656	34, −23, 60	Right SM
			1303	−28, −25, 62	Left SM
			848	1, −17, 53	Bilateral SMA/CC
Right V	738	696 (94.31%)	622	−31, −23, 61	Left SM
			27	−2, −16, 52	Left SMA/CC
Left VI	1561	1436 (92%)	1546	50, −40, 43	Right IPL
			455	−60, −34, 35	Left IPL
			1005	37, 46, 23	Right MFG
			494	−37, 43, 26	Left MFG
			987	44, 13, 6	Right IFG/INS
			501	−39, 9, 5	Left INS
			604	3, 17, 38	Bilateral CC
			136	25, 7, 61	Right PM
			104	56, −54, −3	Right OTC
Right VI	1418	1274 (98.84%)	1168	−40, 42, 17	Left MFG
			1045	−46, 11, 13	Left IFG/INS
			76	43, 7, 1	Right INS
			475	−4, 18 42	Bilateral CC
			364	−49, −42, 46	Left IPL
			139	−14, 5, 69	Left PM
			27	−54, −60, −4	Left OTC
Left VIIIa	847	426 (50.30%)	2423	54, −13, 18	Right TPJ
			1955	−54, −17, 17	Left TPJ
			1900	4, −2, 55	Bilateral CC/PM
			1659	23, −50, 63	Right SPL
			897	−22, −49, 64	Left SPL
			318	−2, −85, 28	Bilateral OCC
			135	53, −61, 1	Right OTC
			65	−51, −67, 4	Left OTC
			119	28, −82, 31	Right OCC
Right VIIIa	798	356 (44.61%)	4155	−49, −13, 28	Left TPJ
			2380	55, −9, 18	Right TPJ
			2151	3, 2, 51	Bilateral CC
			1528	−25, −51, 61	Left SPL
			1189	24, −50, 63	Right SPL
			309	−46, −72, 5	Left OTC
			87	54, −63, 1	Right OTC
			66	−5, −85, 36	Left OCC
			54	21, −82, 40	Right OCC
Left VIIIb	712	183 (25.70%)	1040	22, −46, 65	Right SPL
			588	−21, −48, 66	Left SPL
			337	3, −5, 52	Bilateral CC
			227	58, −25, 30	Right TPJ
			206	−51, −29, 20	Left TPJ
			171	20, −7, 68	Right PM
			69	55, −64, 1	Right OTC
Right VIIIb	697	198 (28.41%)	2922	−35, −37, 49	Left SPL/TPJ
			1412	21, −47, 64	Right SPL
			581	56, −22, 23	Right TPJ
			588	1, −8, 52	Bilateral CC
			461	−20, −12, 67	Left PM
			158	25, −10, 63	Right PM
			139	−49, −74, 5	Left OTC
			42	53, −63, 0	Right OTC

*before erosion/dilation; A voxel has a volume of 2 mm³; aROIs, anatomical regions of interest; fROIs, functional regions of interest; CC, cingulate cortex; IFG, inferior frontal gyrus; INS, insula; IPL, inferior parietal lobe; MFG, middle frontal cortex; PM, premotor cortex; OCC, extrastriate areas of occipital cortex; OTC, occipito-temporal cortex; SMA, supplementary motor cortex; SM, pre- and postcentral gyrus; SPL, superior parietal lobe; TPJ, temporo-parietal junction.

Table 2 contains the thalamic center-of-mass (CoM) coordinates and their probability of belonging to a structurally defined thalamic region based on the Thalamic Connectivity Atlas (Johansen-Berg et
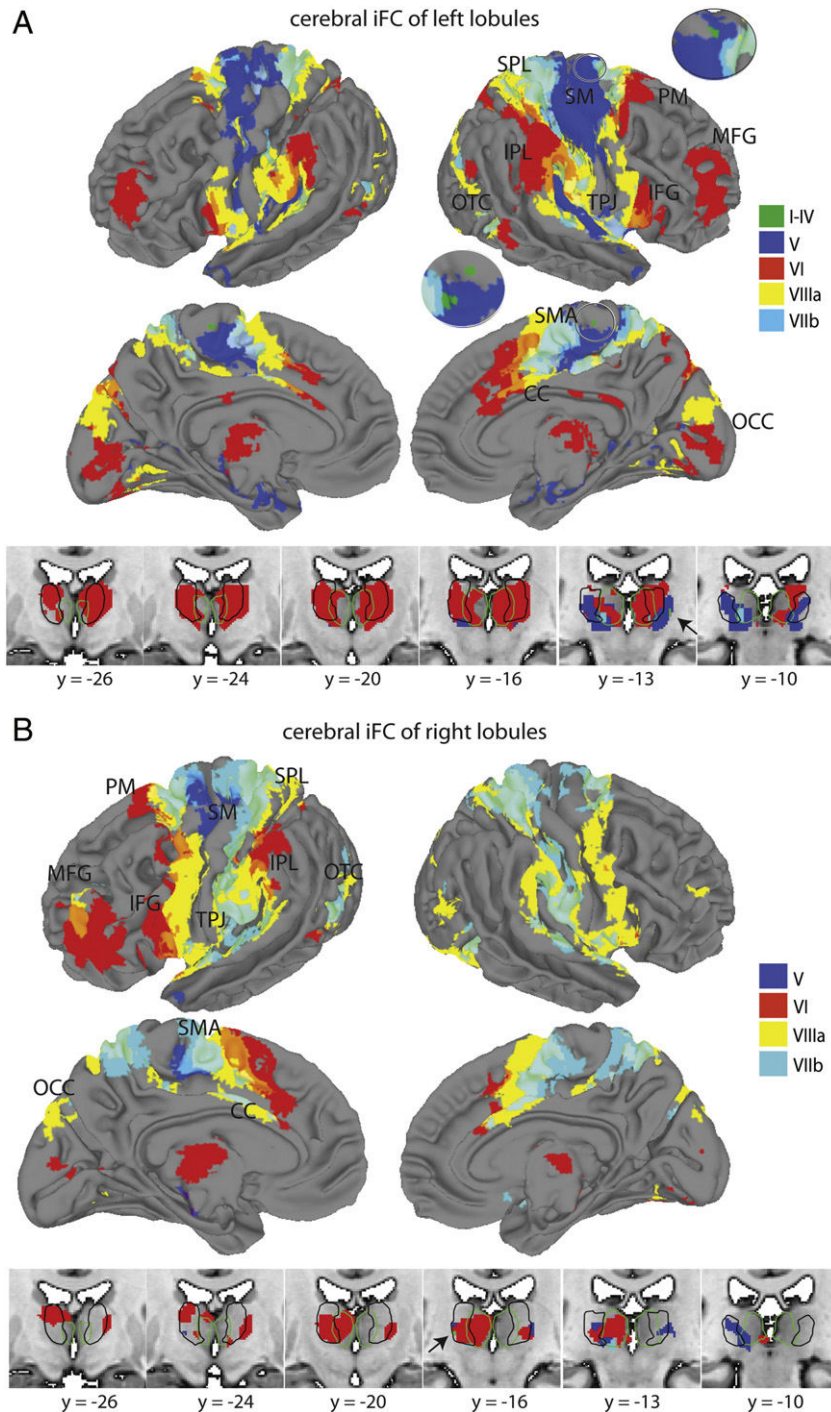
Fig. 3. iFC maps based on the five different fROIs in each hemisphere. Thresholded and color-coded cerebral connectivity patterns are represented on partially inflated cerebral surface maps. Cerebral overlaps are displayed by means of translucent colors. (A) displays cerebral iFC maps of left cerebellar lobules I–IV, V, VI, and VIIIa/b (top) and corresponding color-coded thalamic maps (bottom). (B) shows iFC maps of right cerebellar lobules V, VI, and VIIIa/b (top) and corresponding color-coded thalamic maps (bottom). Left lobules I–IV are connected to bilateral ventral primary sensorimotor areas, which are displayed in the enlarged circles. Left lobule V is connected to bilateral primary sensorimotor cortex (SM), supplementary motor cortex (SMA), and cingulate cortex (CC). Right lobule V is connected to left SM, and left SMA/CC. Left lobule VI is connected to bilateral inferior and middle frontal gyrus (IFG/MFG), bilateral superior and inferior posterior parietal lobe (IPL/SPL), occipito-temporal gyrus (OTC), bilateral medial prefrontal cortex (mPFC), CC, and right premotor cortex (PM). Right lobule VI shows iFC to left MFG, IFG, PM, IPL, mPFC/CC, and bilateral OCC. Left and right lobule VIIIa shows iFC to temporo-parietal junction (TPJ), OTC, SPL, PM, and mPFC/CC, OCC. Left and right lobule VIIIb is connected to SPL, TPJ, PM, mPFC/CC, OTC, OCC. Right lobule VIIIb also shows connectivity to left MFG. Color-coded regions within the thalamus are displayed below on six slices. The outlines represent the group of medial (green) and lateral (black) thalamic nuclei according to the Morel et al. (1997). The arrows indicate the thalamic connectivity of left and right I–IV.

al., 2005) as well as a medial or lateral group of thalamic nuclei as defined by a multiarchitectonic atlas (Morel et al., 1997). In addition we report the connectivity to subcortical structures. Unthresholded contrast images of the weighted-ANOVA are presented in Supplementary Fig. 3.

Lobules I–IV

The iFC pattern of left lobules I–IV included ventral parts of the precentral gyrus (SM) and the brain stem. The iFC of right and left lobules I–IV was found in cross-lateralized lateral thalamus.

Table 2

Connectivity to thalamic and subcortical areas of cerebellar lobules I–IV, V, VI, and VIIIa. Center of mass coordinates for thalamic regions are reported, along with the closest distance to medial or lateral thalamic nuclei of the Morel atlas, as well as the probabilistic connectivity to cerebral areas of these thalamic coordinates according to the Oxford thalamic atlas. CA, caudate; GP, globus pallidus; M, primary motor cortex; PFC, pre-frontal cortex; PM, pre-motor cortex; PP, posterior-parietal cortex; PU, putamen; S, sensory cortex.

Lobule	Coordinates (x, y, z)	Thalamic REGION	Probabilistic cerebral connectivity	Subcortical regions
Right I–IV	−18, −19, 4	Lateral –	65% M, 35% PM –	–
Left I–IV	20, −20, 2	Lateral –	50% S, 39% M –	Brain stem
Right V	−14, −21, 3	Lateral	59% M, 38% S	Bilat. PU, bilat. GP, brain stem
Left V	16, −19, 4	Lateral	45% PM, 41% M	
	15, −21, 3	Lateral	59% M, 38% M	Bilat. PU, bilat. GP, brain stem
Right VI	−13, −22, 2	Lateral	48% PM, 37% M	
	−9, −14, 8	Lateral	93% PFC	Bilat. CA, bilat. PU, bilat. GP, brain stem
Left VI	14, −10, 7	Lateral	76% PFC, 26% PM	
	10, −14, 8	Lateral	90% PFC	Bilat. CA, bilat. PU, bilat. GP, brain stem
Right VIIIa	−11, −13, 8	Lateral	93% PFC	
	−10, −21, −2	Medial	36% PM, 36% M	–
Left VIIIa	–	–	–	–
	14, −23, 3	Lateral	34% S, 31% PP	–
	−12, −23, 2	Medial	44% M, 31% PP	

Lobule V

Left lobule V was connected to regions within the bilateral sensorimotor cortex engulfing pre- and postcentral areas (SM), bilateral supplementary motor area (SMA), and cingulate cortex (CC). iFC of right lobule V was found in the left SM, SMA/CC. Left and right lobule V included iFC to brainstem, bilateral lateral thalamus, bilateral globus pallidus, and putamen (extending into the insular cortex).

Lobule VI

Left lobule VI connectivity was found in the bilateral middle frontal gyrus (MFG), bilateral inferior frontal gyrus (IFG; with extension towards the insular cortex), right premotor cortex (PM), bilateral inferior parietal lobe (IPL), bilateral occipito-temporal cortex (OTC), as well as in bilateral medial occipital cortex (OCC). Right lobule VI was connected to left MFG, left IFG (with extension towards the insular cortex), left PM, left IPL, left OTC, and bilateral OCC. Both left and right lobule VI showed iFC to bilateral CC and medial prefrontal cortex (mPFC) as well as subcortical connections including bilateral lateral thalamus, caudate, putamen, globus pallidus, and brain stem.

Lobule VIIIa

iFC of left and right lobule VIIIa was found in bilateral superior parietal lobe (SPL), bilateral temporo-parietal junction (TPJ), bilateral CC/mPFC, which extended bilaterally towards PM, bilateral OTC, and bilateral OCC. Subcortical iFC was found in left lateral thalamus (right VIIIa) and bilateral lateral thalamus (left VIIIa).

Lobule VIIIb

iFC of left and right lobule VIIIb was found in bilateral SPL, TPJ, PM, mPFC/CC, and OTC. No subcortical iFC was found for either left or right lobule VIIIb.

We also performed the same analysis with aROIs (instead of fROIs) and carried out a two-way ANOVA in which we contrasted the iFC maps of fROIs and aROIs. Despite high connectivity between cerebellar homologs, connectivity that was lobular-specific and not mirrored by the signal in the homologous lobule might be superimposed by stronger connectivity to one of the adjacent cerebral areas. The cerebello-cerebral signal separation excluded these voxels and might have been overly conservative. However, the direct contrast between aROIs and fROIs revealed that mainly noise-susceptible areas showed decreases in connectivity. In Supplementary Fig. 4 we show decreased iFC in areas proximate to CSF, air, skull, the interhemispheric fissure and the transverse and frontal sinuses, when using fROIs. Further, cerebral areas in parietal and prefrontal cortex, which have been found to be contaminated by physiological signal, also showed a decrease in iFC (Tong et al., 2011). Increases in iFC using fROIs were found in subcortical areas such as thalamus, midbrain and basal ganglia as well as in cortical areas. These findings can be taken as an indication that fROIs improve the functional relevance of cerebellar lobules.

*Overlapping and separate topography of cerebral regions in the cerebellum*

The detailed voxelwise correlation analysis between 18 cerebral clusters, which were defined based on the initial iFC analysis, and voxels within cerebellar fROIs, determined cerebellar mapping of separate and overlapping cerebral connectivity (Fig. 4). The cerebral clusters used in the partial correlation analysis included for left and right lobule V: SM and CC; lobule VI: IPL, MFG, IFG, OTC, CC, and PM; lobule VIIIa: TPJ, SPL, CC, OTC, and two regions in the OCC; and lobule VIIIb: SPL/TPJ, CC, PM, and OTC. For left and right lobules I–IV, no cluster survived the erosion/dilation procedure. The CoM coordinates and sizes of cerebral clusters are represented in Table 1.

Cerebellar voxels which showed connectivity from overlapping mPFC/CC regions of lobules V, VI, and VIIIa/b were collapsed (purple color in Fig. 4B). Partially overlapping parietal areas (temporo-parietal and posterior-parietal regions), which were connected with lobules VI and VIIIa/b were grouped together (Fig. 4B, cyan color). Connectivity of occipital and overlapping premotor regions were also grouped, but did not survive the threshold and are not represented in the cerebellar map. Supplementary Table 1 includes the 13 and 28 different cerebral cluster combinations for left and right cerebellar hemispheres respectively, and demonstrates how they were color-coded in Fig. 4B.

The mapping of left cerebellar regions I–X showed distributed connectivity from parietal regions (35% of the entire cerebellar hemispheric fROIs), middle frontal cortex (16%), cingulate regions (13%), overlapping sensorimotor, cingulate, occipito-temporal and parietal regions (12%), sensorimotor regions (11%), overlapping sensorimotor, occipito-temporal, and parietal regions (4%), occipito-temporal (3%), overlapping occipito-temporal and parietal regions (3%), overlapping cingulate and parietal regions (2%), and overlapping middle frontal cortex and cingulate regions (1%).

In the right cerebellar hemisphere we identified connectivity from sensorimotor regions (30% of the entire cerebellar hemispheric fROIs), middle frontal cortex (23%), overlapping sensorimotor, cingulate, occipito-temporal and parietal regions (14%), overlapping sensorimotor, prefrontal, occipito-temporal, and parietal regions (9%), cingulate regions (8%), overlapping sensorimotor, occipito-temporal, and parietal regions (6%), parietal regions (2%), overlapping middle frontal and parietal regions (2%), overlapping inferior frontal, cingulate, parietal, and occipito-temporal regions (2%), occipito-temporal regions (1%), overlapping middle frontal and cingulate regions (1%) and other combinations of cerebral connectivity (<1%).

Lobularwise, in left lobules I–V we found separate iFC from the sensorimotor cortex, cingulate, and occipito-temporal regions, which overlapped partially with parietal regions. Separate and overlapping iFC of cingulate and sensorimotor extended towards the superior
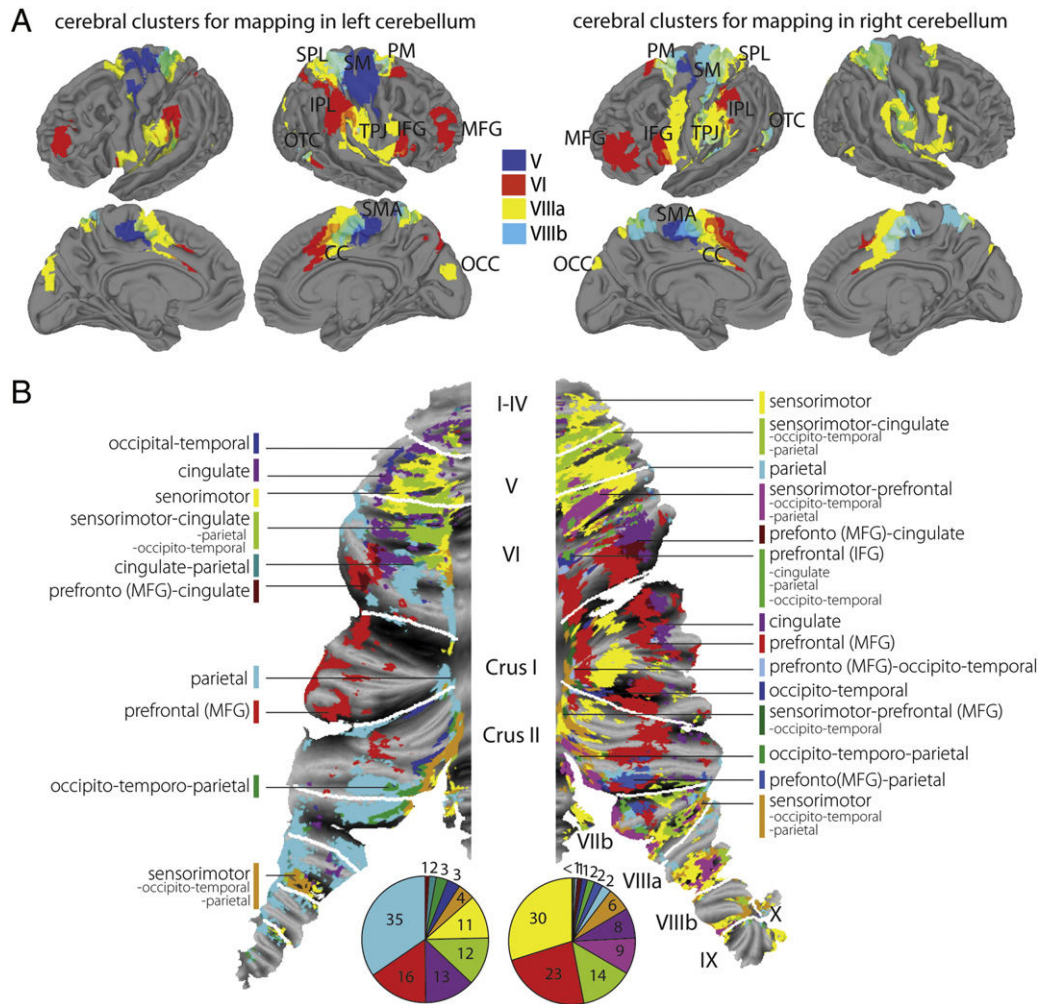
Fig. 4. (A) represents thresholded, eroded, dilated and color-coded 18 cerebral clusters of voxelwise cerebello-cerebral iFC analysis (Fig. 3) overlaid on partially inflated cerebral surface maps. Cerebral overlaps are displayed by means of translucent colors. (B) displays cerebral connectivity across the entire cerebellum according to the colored lines along with a description of the connected cerebral regions (p < 0.00001, voxelwise FDR corr.). The color-coded pie charts at the bottom represent the cerebral connectivity distribution for each cerebellar hemisphere (in percentage).

portion of left lobule VI and along medially regions in left lobules II and VIIIb. In right lobules I–V iFC of sensorimotor regions were separate from and overlapping with iFC from cingulate, occipito-temporal and parietal regions. Separate and overlapping sensorimotor iFC extended in superior regions of lobule VI, medial regions of right lobules Crus I and Crus II as well as in lobules VIIb and VIIIa/b. The inferior portions of left lobule VI showed additionally iFC from the middle frontal cortex laterally, extending towards lobules Crus I and Crus II. iFC from parietal regions was present mainly in medial regions and continued in lobules Crus I, Crus II, VIIb, and VIIIa/b. iFC of prefrontal and parietal regions partly overlapped with iFC from cingulate regions. Right lobule VI showed separate and overlapping iFC from the middle frontal cortex, and laterally from the cingulate regions, which extend towards lobule Crus I. In the superior portion of right lobule VI overlapping iFC from sensorimotor, prefrontal, occipito-temporal, and parietal regions as well as a narrow horizontal strand of separate and overlapping iFC from inferior frontal with cingulate, parietal, and occipito-temporal regions was found.

In left lobules VIIIa/b, iFC from sensorimotor and parietal was found to be separate and overlapping with occipito-temporal regions as well as separate iFC of cingulate regions. In right lobules VIIIa/b sensorimotor iFC was found to be separate and overlapping with prefrontal, parietal, cingulate, occipito-temporal as well as separate parietal iFC.

Discussion

Cerebello-cerebral functional subsystems

The cerebellum has been found to play a pivotal role not only in primary sensorimotor processes but also in higher-order sensorimotor, cognitive and affective function. Based on our findings, we present a sublobular topography of functional cerebello-cerebral systems. Using information from both cerebral and cerebellar mapping we identified cerebellar subsystems that go beyond anatomical borders. The function of those subsystems is based on the function of the cerebral areas they implicated: an affective and a cognitive control network (cingulate cortex and medial prefrontal cortex), a motor control network (primary sensorimotor cortex), a multisensory network (secondary sensorimotor areas, temporo-parietal junction, occipito-temporal cortex), and a cognitive executive network (inferior/middle frontal gyrus). Given the lack of task-based information in this study, this organization of cerebello-cerebral systems currently over-simplifies the functions of the underlying anatomical structures. The cerebellar mapping represents an approximation of how cerebral connectivity is organized on a sublobular level as it is determined by a statistical threshold. However, the contribution of such a detailed cerebellar mapping has implications for models of action control. We discuss the role of the cerebellum with

respect to the cerebral networks and present evidence for cross-lobular integration of network information at the cerebellar level.

Cerebellar affective and cognitive control system

A cerebellar contribution to motivation and intention (Devinsky et al., 1995), error monitoring (Shane et al., 2008), and autonomic functions such as cardiovascular control of stressors (Critchley et al., 2000) and emotional processing (Devinsky et al., 1995; Schmahmann et al., 2007; Stoodley and Schmahmann, 2009) is supported by the anatomical connectivity between cingulate cortex and pontine nuclei in macaque monkeys (Glickstein et al., 1985; Schmahmann and Pandya, 1997; Vilensky and van Hoesen, 1981). Our results extend the view of cerebello-cingulate interaction and implicate a strong connectivity between mPFC/CC and lobules V, VI and VIIIa/b. Using seed based iFC analysis Margulies et al. (2007) showed that anterior CC regions (s3 and s4), which are in the vicinity of the lobule VI-connected CC region, are connected to the prefrontal and inferior parietal cortex. Lobules VIIIa/b-connected CC regions were connected to a fronto-parietal network involved in sensorimotor processes (regions s1–s2). When we decreased the threshold for lobule V (p < 0.01, FDR corr.), we found a caudal anterior CC region, which is associated with affective processes (region i5). At the cerebellar level, the strong lateral as well as widespread overlapping cingulate connectivity with sensorimotor, multisensory, and cognitive executive systems might demonstrate an integration of affective/cognitive control information to various stages during action performances, conflict detection, and error-driven motor learning (Lehericy et al., 2005; Margulies et al., 2007). Note that in the current study only a subset of cerebellar regions were investigated and shown to be connected to areas involved in affective and cognitive processes. In addition, parts of posterior cerebellar lobules are also connected to the cerebral limbic system (Schmahmann, 2004).

Cerebellar sensorimotor system

As expected, cerebellar lobules I–V showed connectivity to the pre- and postcentral cortex, as well as SMA/CC and lateral thalamic regions which are connected to primary sensorimotor regions. The cerebello-thalamic connectivity was recently shown using fiber tracking in humans (Salmi et al., 2010). While lobules I–IV were connected to ventral primary motor areas, representing the leg area, lobule V was connected to dorsal primary motor cortex (Buckner et al., 2011; Grodd et al., 2001), representing the upper body. A recruitment of lobule V has also been described during state-dependent coordination, where predictive state values of one effector enable the coordination of another (Diedrichsen et al., 2007). The cerebellar mapping of cerebral connectivity reveals also a contribution of lobules VI, Crus I, Crus II, VIIb, and VIIIa/b to sensorimotor processes, which is supported by tract-tracing in animals (Kelly and Strick, 2003; Lu et al., 2007). Lobule VI has been shown to represent the tongue and lips in humans (Buckner et al., 2011; Grodd et al., 2001). To what extent the connectivity to SMA is driven by the cerebellum (lobules V/VI) or by basal ganglia is unclear, as both structures are interconnected (Bostan and Strick, 2010) and are targeted by the SMA (Akkal et al., 2007).

Lobules VIIIa/b were found to be connected to primary and secondary sensorimotor thalamic (only lobule VIIIa) and cerebral regions. This is in line with iFC studies (Buckner et al., 2011; Krienen and Buckner, 2009; O'Reilly et al., 2010) and task fMRI (Grodd et al., 2001; Stoodley and Schmahmann, 2010; Wiestler et al., 2011). The first cerebello-cerebral iFC analysis revealed connectivity of lobules VIIIa/b to secondary sensory, premotor, cingulate, and occipito-temporal areas, but not primary motor cortex. This suggests an additional role of lobules VIIIa/b in higher-order processes (Prevosto et al., 2010). Furthermore, according to Schmahmann (2007) lesions in the posterior lobules VII–

X do not lead to cerebellar motor syndrome as compared to anterior lobules I–V.

The overlap of sensorimotor with parietal and occipito-temporal connectivity in cerebellar bilateral lobules I–V and VI, along the midline of lobules Crus I and II, left VIIIa, and right VIIb–IX provides evidence for internal models of proprioception as well as visually derived information, which allow for the coordination of movements towards targets (Ramnani et al., 2001) and goal-directed action (Shadmehr and Krakauer, 2008). However, in future connectivity studies the weight of primary and secondary sensorimotor connectivity to these regions should be addressed in detail.

Lobule VIIIb lacked connectivity to subcortical regions, which was also absent in a study of diffusion-weighted imaging that did not find fiber tracks between lobule VIII and thalamic endpoints (Salmi et al., 2010). As the ventral thalamus receives efferent connections from the dentate nucleus and projects to parietal regions, thalamic connectivity of lobule VIIIb might be weak comparable to the signal of the other lobules. Furthermore, the low SNR in particularly the inferior lobules VIIIb might have influenced the cerebello-cerebral signal separation and subsequent iFC results.

Lobules I–IV also posed a methodological concern, as the masks in each hemisphere contained four adjacent lobules. This was due to the inability to distinguish the lobules given the comparatively low spatial resolution of the data. The heterogeneity of the extracted signal may have weakened connectivity to primary motor areas, especially in right lobules I–IV (see unthresholded iFC maps in Supplementary Fig. 3). In the future, higher resolution functional images would be required to segment cerebellar lobules I–IV and to accurately distinguish their connectivity patterns.

Cerebellar multisensory system

The strong connectivity of posterior parietal connectivity throughout the entire cerebellum, and particularly in the left cerebellum, stresses the substantial contribution to the integration of contextual information from various proprioceptive sources for coordinating and integrating the dynamics of targets and executed movements as shown in animal and human studies (Prevosto et al., 2010; Stein and Glickstein, 1992) as well as in recalibrating sensory representations during motor adaptation (Clower et al., 2001). In addition, a strong occipito-temporal iFC, prominently overlapping with iFC from sensorimotor, prefrontal, and parietal regions in bilateral lobules I–VI, Crus II, VIIb, VIIIa, and right lobules Crus I, VIIIb, and IX might be attributed to various visuomotor coordinatory processes as well as visual tracking of motion (Miall et al., 2000; Sokolov et al., 2012; Stein and Glickstein, 1992). In the primate brain, ponto-cerebellar connectivity has been found to mediate visual processes (Brodal, 1979; Glickstein et al., 1994) from the occipito-temporal as well as parietal cortex (Schmahmann and Pandya, 1991). This overlapping connectivity might be also particularly important for a language-related visual system in reading and writing, auditory processes, as well as articulation (Stoodley and Stein, 2013).

Cerebellar control system

In humans, the cerebellar lobules VI, Crus I, and Crus II have been implicated in executive functions such as selecting stored internal models after acquired tool use (Imamizu and Kawato, 2012; Imamizu et al., 2000), task accomplishment (Ramnani, 2012), working memory, verb generation and fluency, and set shifting (Schmahmann et al., 2007; Stoodley et al., 2012). As revealed by a meta-analysis and a seed-based iFC analysis, middle and inferior frontal gyri are part of a network – which resembled the network involving lobule VI – being responsible for working memory, flexibility, inhibition, and language (Sundermann and Pfleiderer, 2012). These large-scale executive networks, which are connected to contralateral cerebellar lobules VI,

Crus I and Crus II (Habas, 2012), involve posterior parietal and prefrontal regions.

In this study the connectivity profiles of parietal and prefrontal regions within the cerebellum appeared to be asymmetrically distributed. First, we observed stronger connectivity of the prefrontal regions in the right cerebellum, whereas parietal were connected strongly to regions in the left hemisphere. Recent work by Wang et al. (2013) suggests that an asymmetry in the cerebellum can be explained by the lateralization of the cerebrum. They demonstrated that the right cerebellar lobules VI, Crus I and II are highly lateralized according to a lateralized cerebral network comprising left inferior frontal gyrus, superior temporal gyrus and temporal pole. Left cerebellar regions were connected to a right cerebral network of insula, parietal operculum and angular gyrus. Secondly, in the left cerebellar hemisphere we found that parietal regions were connected stronger to medial cerebellar regions in lobules Crus I, Crus II, and VIIb, whereas prefrontal regions were connected more to lateral areas in lobules VI and Crus I. In nonhuman primates, posterior parietal regions have been found to be connected to translobular bands along the medial cerebellum spanning lobules V, VI, Crus I, and VIIb (Prevosto et al., 2010). Kelly and Strick (2003) demonstrated that prefrontal connectivity occurs mainly along lateral portions of lobules Crus I, Crus II, VIIb and IX.

Even though left and right cerebellar mapping was generated from cerebral clusters that were connected to both left and right cerebellar homologs, they varied in size and laterality. It is beyond the scope of this study to statistically validate the extent to which prefronto-parietal separation represents distinct functional sublobular zones, or whether this connectivity is lateralized. However, this detailed mapping shows that cerebellar lobules consist of homogeneous sublobular functional zones which show specifically stronger connectivity for different cerebral regions.

Methodological approaches to study cerebellar connectivity

Restriction of the anatomical regions to relevant voxels substantially increased its functional specificity. The functional definition within anatomical ROIs is beneficial for capturing meaningful iFC of cerebello-cerebral networks. Especially when for group-level analysis a certain region is not transformed to a region-only template, but to a global template as the entire brain, the smoothness inherent by normalization leads to distorted connectivity. This is crucial because brain regions are often in the vicinity of functionally unrelated anatomical structures. Thus, functional separation also offers a more general possibility for defining other brain structures as well. We used visual and parahippocampal structures as cerebral reference regions for all lobules. A different reference region may have improved the cerebellar signal in lobule VIIIb, as it is more adjacent to CSF and the brainstem.

Unique connectivity patterns of every cerebellar lobule were presented based on results of a weighted-ANOVA. The main effect of each lobule by itself yielded rather global and non-specific cerebral iFC patterns (data not shown). The removal of common variance was found to be a crucial step in determining cerebello-cerebral iFC patterns. Only for the thalamus, the main effects of cerebellar regions revealed strong connectivity for every lobule (Supplementary Fig. 5).

iFC results likely include direct cerebro-subcortico-cerebellar connectivity as well as indirect cerebro-cerebral and cerebro-subcortical connectivity. In this study we have addressed the influence of third parties by means of partial correlation. However, partial correlation was performed between cerebral regions that were connected to a single lobule, but not between regions connected to different lobules. Adjacent regions such as superior parietal lobe (connected to lobules VIIIa/b) and primary sensorimotor cortex (connected to lobules IV/V) might have common variance that was not accounted for in this study.

For the cerebellar mapping we only represent the spatial distribution of the strongest cerebral connectivity, as this is clearly dependent on the chosen threshold. As we only selected highly connected cerebral and cerebellar regions, we cannot rule out false negatives, but can rather assess differential connectivity to sublobular regions (as presented in Fig. 4B). To what extent the amount of overlap or the weight at each cerebellar voxel demonstrates unique input requires further research with the use of high-resolution data.

Even though the representation of a cerebellar flat map optimizes visualization, the spatial correspondence remains an approximation of anatomical correspondence due to the rather low-resolution that underlies the surface reconstruction. The low resolution of the functional data ($3 \times 3 \times 4$ mm) might have additionally influenced the spatial distribution. Studies of higher resolution data are required to not only obtain more anatomical precision, but also to provide better visualization of the intricate cerebellar surface.

Conclusion

Methodological challenges inherent in studying the densely folded cerebellum with fMRI should be carefully considered in order to develop methods to reveal detailed cerebello-cerebral network information. We have identified five cerebellar lobules involved in action control, and described their separate (lobules I–IV, V, VI) as well as overlapping (lobules VIIIa/b) cerebral connectivity. The cerebral clusters, that we have found to be involved in action control, however, seem to be unevenly distributed across and within cerebellar lobules. A spatially distinct as well as overlapping topography of sensorimotor, parietal, prefrontal, occipito-temporal and cingulate connectivity suggest a sublobular functional organization, which confirms models that extend organization beyond the anatomical lobular divisions (Buckner et al., 2011). Taken together, the detail of this cerebellar mapping shows a functionally overlapping and parallelized cerebral topography that spans multiple lobules. The findings of functionally distinct areas within and across lobules increase our understanding of its spatial organization, and provide a basis for functional parcellation that is independent of anatomical divisions. However, higher-resolution data are clearly necessary to understand and utilize the cross-lobular arrangement of cerebral connectivity as well as how these network interactions represent the underlying key processes of motor behavior.

Funding

Conflict of interest

None declared.

Appendix A. Supplementary data

Supplementary data to this article can be found online at http://dx.doi.org/10.1016/j.neuroimage.2013.07.027.

References

Akkal, D., Dum, R.P., Strick, P.L., 2007. Supplementary motor area and pre-supplementary motor area: targets of basal ganglia and cerebellar output. J. Neurosci. 27, 10659–10673.

Allen, G.I., Azzena, G.B., Ohno, T., 1974. Somatotopically organized inputs from fore- and hindlimb areas of sensorimotor cortex to cerebellar Purkyne cells. Exp. Brain Res. 20, 255–272.

Blakemore, S.J., Wolpert, D.M., Frith, C.D., 1998. Central cancellation of self-produced tickle sensation. Nat. Neurosci. 1, 635–640.

Bostan, A.C., Strick, P.L., 2010. The cerebellum and basal ganglia are interconnected. Neuropsychol. Rev. 20, 261–270.

Brodal, P., 1979. The pontocerebellar projection in the rhesus monkey: an experimental study with retrograde axonal transport of horseradish peroxidase. Neuroscience 4, 193–208.

Buckner, R.L., Krienen, F.M., Castellanos, A., Diaz, J.C., Yeo, B.T., 2011. The organization of the human cerebellum estimated by intrinsic functional connectivity. J. Neurophysiol. 106, 2322–2345.

Clower, D.M., West, R.A., Lynch, J.C., Strick, P.L., 2001. The inferior parietal lobule is the target of output from the superior colliculus, hippocampus, and cerebellum. J. Neurosci. 21, 6283–6291.

Courchesne, E., Allen, G., 1997. Prediction and preparation, fundamental functions of the cerebellum. Learn. Mem. 4, 1–35.

Cox, R.W., 1996. AFNI: software for analysis and visualization of functional magnetic resonance neuroimages. Comput. Biomed. Res. 29, 162–173.

Critchley, H.D., Corfield, D.R., Chandler, M.P., Mathias, C.J., Dolan, R.J., 2000. Cerebral correlates of autonomic cardiovascular arousal: a functional neuroimaging investigation in humans. J. Physiol. 523 (Pt 1), 259–270.

Cui, S.Z., Li, E.Z., Zang, Y.F., Weng, X.C., Ivry, R., Wang, J.J., 2000. Both sides of human cerebellum involved in preparation and execution of sequential movements. Neuroreport 11, 3849–3853.

Desikan, R.S., Segonne, F., Fischl, B., Quinn, B.T., Dickerson, B.C., Blacker, D., Buckner, R.L., Dale, A.M., Maguire, R.P., Hyman, B.T., Albert, M.S., Killiany, R.J., 2006. An automated labeling system for subdividing the human cerebral cortex on MRI scans into gyral based regions of interest. NeuroImage 31, 968–980.

Devinsky, O., Morrell, M.J., Vogt, B.A., 1995. Contributions of anterior cingulate cortex to behaviour. Brain 118 (Pt 1), 279–306.

Diedrichsen, J., 2006. A spatially unbiased atlas template of the human cerebellum. NeuroImage 33, 127–138.

Diedrichsen, J., Criscimagna-Hemminger, S.E., Shadmehr, R., 2007. Dissociating timing and coordination as functions of the cerebellum. J. Neurosci. 27, 6291–6301.

Diedrichsen, J., Balsters, J.H., Flavell, J., Cussans, E., Ramnani, N., 2009. A probabilistic MR atlas of the human cerebellum. NeuroImage 46, 39–46.

Glickstein, M., May III, J.G., Mercier, B.E., 1985. Corticopontine projection in the macaque: the distribution of labelled cortical cells after large injections of horseradish peroxidase in the pontine nuclei. J. Comp. Neurol. 235, 343–359.

Glickstein, M., Gerrits, N., Kralj-Hans, I., Mercier, B., Stein, J., Voogd, J., 1994. Visual pontocerebellar projections in the macaque. J. Comp. Neurol. 349, 51–72.

Grodd, W., Hulsmann, E., Lotze, M., Wildgruber, D., Erb, M., 2001. Sensorimotor mapping of the human cerebellum: fMRI evidence of somatotopic organization. Hum. Brain Mapp. 13, 55–73.

Habas, C., 2012. Functional imaging and the cerebellum: recent developments and challenges. Editorial. Cerebellum 11, 311–313.

Habas, C., Cabanis, E.A., 2008. Neural correlates of simple unimanual discrete and continuous movements: a functional imaging study at 3 T. Neuroradiology 50, 367–375.

Habas, C., Axelrad, H., Cabanis, E.A., 2004. The cerebellar second homunculus remains silent during passive bimanual movements. Neuroreport 15, 1571–1574.

Habas, C., Kamdar, N., Nguyen, D., Prater, K., Beckmann, C.F., Menon, V., Greicius, M.D., 2009. Distinct cerebellar contributions to intrinsic connectivity networks. J. Neurosci. 29, 8586–8594.

Hampson, M., Peterson, B.S., Skudlarski, P., Gatenby, J.C., Gore, J.C., 2002. Detection of functional connectivity using temporal correlations in MR images. Hum. Brain Mapp. 15, 247–262.

Holmes, G., 1939. The cerebellum of man. Brain 62, 1–30.

Hulsmann, E., Erb, M., Grodd, W., 2003. From will to action: sequential cerebellar contributions to voluntary movement. NeuroImage 20, 1485–1492.

Imamizu, H., Kawato, M., 2012. Cerebellar internal models: implications for the dexterous use of tools. Cerebellum 11, 325–335.

Imamizu, H., Miyauchi, S., Tamada, T., Sasaki, Y., Takino, R., Putz, B., Yoshioka, T., Kawato, M., 2000. Human cerebellar activity reflecting an acquired internal model of a new tool. Nature 403, 192–195.

Jancke, L., Specht, K., Mirzazade, S., Peters, M., 1999. The effect of finger-movement speed of the dominant and the subdominant hand on cerebellar activation: a functional magnetic resonance imaging study. NeuroImage 9, 497–507.

Johansen-Berg, H., Behrens, T.E., Sillery, E., Ciccarelli, O., Thompson, A.J., Smith, S.M., Matthews, P.M., 2005. Functional–anatomical validation and individual variation of diffusion tractography-based segmentation of the human thalamus. Cereb. Cortex 15, 31–39.

Jueptner, M., Ottinger, S., Fellows, S.J., Adamschewski, J., Flerich, L., Muller, S.P., Diener, H.C., Thilmann, A.F., Weiller, C., 1997. The relevance of sensory input for the cerebellar control of movements. NeuroImage 5, 41–48.

Kelly, R.M., Strick, P.L., 2003. Cerebellar loops with motor cortex and prefrontal cortex of a nonhuman primate. J. Neurosci. 23, 8432–8444.

Krienen, F.M., Buckner, R.L., 2009. Segregated fronto-cerebellar circuits revealed by intrinsic functional connectivity. Cereb. Cortex 19, 2485–2497.

Lehericy, S., Benali, H., Van de Moortele, P.F., Pelegrini-Issac, M., Waechter, T., Ugurbil, K., Doyon, J., 2005. Distinct basal ganglia territories are engaged in early and advanced motor sequence learning. Proc. Natl. Acad. Sci. U. S. A. 102, 12566–12571.

Lu, X., Miyachi, S., Ito, Y., Nambu, A., Takada, M., 2007. Topographic distribution of output neurons in cerebellar nuclei and cortex to somatotopic map of primary motor cortex. Eur. J. Neurosci. 25, 2374–2382.

Manto, M., Bower, J.M., Conforto, A.B., Delgado-Garcia, J.M., da Guarda, S.N., Gerwig, M., Habas, C., Hagura, N., Ivry, R.B., Marien, P., Molinari, M., Naito, E., Nowak, D.A., Oulad Ben Taib, N., Pelisson, D., Tesche, C.D., Tilikete, C., Timmann, D., 2012. Consensus paper: roles of the cerebellum in motor control—the diversity of ideas on cerebellar involvement in movement. Cerebellum 11, 457–487.

Margulies, D.S., Kelly, A.M., Uddin, L.Q., Biswal, B.B., Castellanos, F.X., Milham, M.P., 2007. Mapping the functional connectivity of anterior cingulate cortex. NeuroImage 37, 579–588.

Miall, R.C., Imamizu, H., Miyauchi, S., 2000. Activation of the cerebellum in co-ordinated eye and hand tracking movements: an fMRI study. Exp. Brain Res. 135, 22–33.

Middleton, F.A., Strick, P.L., 1997. Cerebellar output channels. Int. Rev. Neurobiol. 41, 61–82.

Middleton, F.A., Strick, P.L., 2000. Basal ganglia and cerebellar loops: motor and cognitive circuits. Brain Res. Brain Res. Rev. 31, 236–250.

Morel, A., Magnin, M., Jeanmonod, D., 1997. Multiarchitectonic and stereotactic atlas of the human thalamus. J. Comp. Neurol. 387, 588–630.

O'Reilly, J.X., Beckmann, C.F., Tomassini, V., Ramnani, N., Johansen-Berg, H., 2010. Distinct and overlapping functional zones in the cerebellum defined by resting state functional connectivity. Cereb. Cortex 20, 953–965.

Orioli, P.J., Strick, P.L., 1989. Cerebellar connections with the motor cortex and the arcuate premotor area: an analysis employing retrograde transneuronal transport of WGA-HRP. J. Comp. Neurol. 288, 612–626.

Prevosto, V., Graf, W., Ugolini, G., 2010. Cerebellar inputs to intraparietal cortex areas LIP and MIP: functional frameworks for adaptive control of eye movements, reaching, and arm/eye/head movement coordination. Cereb. Cortex 20, 214–228.

Ramnani, N., 2012. Frontal lobe and posterior parietal contributions to the cortico-cerebellar system. Cerebellum 11, 366–383.

Ramnani, N., Toni, I., Passingham, R.E., Haggard, P., 2001. The cerebellum and parietal cortex play a specific role in coordination: a PET study. NeuroImage 14, 899–911.

Rijntjes, M., Buechel, C., Kiebel, S., Weiller, C., 1999. Multiple somatotopic representations in the human cerebellum. Neuroreport 10, 3653–3658.

Salmi, J., Pallesen, K.J., Neuvonen, T., Brattico, E., Korvenoja, A., Salonen, O., Carlson, S., 2010. Cognitive and motor loops of the human cerebro-cerebellar system. J. Cogn. Neurosci. 22, 2663–2676.

Sang, L., Qin, W., Liu, Y., Han, W., Zhang, Y., Jiang, T., Yu, C., 2012. Resting-state functional connectivity of the vermal and hemispheric subregions of the cerebellum with both the cerebral cortical networks and subcortical structures. NeuroImage 61, 1213–1225.

Schlerf, J.E., Verstynen, T.D., Ivry, R.B., Spencer, R.M., 2010. Evidence of a novel somatopic map in the human neocerebellum during complex actions. J. Neurophysiol. 103, 3330–3336.

Schmahmann, J.D., 2004. Disorders of the cerebellum: ataxia, dysmetria of thought, and the cerebellar cognitive affective syndrome. J. Neuropsychiatry Clin. Neurosci. 16, 367–378.

Schmahmann, J.D., 2007. The primary motor cerebellum is in the anterior lobe but not the posterior lobe. Evidence from stroke patients. Neurology 68, A357.

Schmahmann, J.D., Pandya, D.N., 1991. Projections to the basis pontis from the superior temporal sulcus and superior temporal region in the rhesus monkey. J. Comp. Neurol. 308, 224–248.

Schmahmann, J.D., Pandya, D.N., 1997. The cerebrocerebellar system. Int. Rev. Neurobiol. 41, 31–60.

Schmahmann, J.D., Doyon, J., McDonald, D., Holmes, C., Lavoie, K., Hurwitz, A.S., Kabani, N., Toga, A., Evans, A., Petrides, M., 1999. Three-dimensional MRI atlas of the human cerebellum in proportional stereotaxic space. NeuroImage 10, 233–260.

Schmahmann, J.D., Weilburg, J.B., Sherman, J.C., 2007. The neuropsychiatry of the cerebellum — insights from the clinic. Cerebellum 6, 254–267.

Scholvinck, M.L., Maier, A., Ye, F.Q., Duyn, J.H., Leopold, D.A., 2010. Neural basis of global resting-state fMRI activity. Proc. Natl. Acad. Sci. U. S. A. 107, 10238–10243.

Shadmehr, R., Krakauer, J.W., 2008. A computational neuroanatomy for motor control. Exp. Brain Res. 185, 359–381.

Shane, M.S., Stevens, M., Harenski, C.L., Kiehl, K.A., 2008. Neural correlates of the processing of another's mistakes: a possible underpinning for social and observational learning. NeuroImage 42, 450–459.

Smaers, J.B., Steele, J., Zilles, K., 2011. Modeling the evolution of cortico-cerebellar systems in primates. Ann. N. Y. Acad. Sci. 1225, 176–190.

Smith, S.M., Jenkinson, M., Woolrich, M.W., Beckmann, C.F., Behrens, T.E., Johansen-Berg, H., Bannister, P.R., De Luca, M., Drobnjak, I., Flitney, D.E., Niazy, R.K., Saunders, J., Vickers, J., Zhang, Y., De Stefano, N., Brady, J.M., Matthews, P.M., 2004. Advances in functional and structural MR image analysis and implementation as FSL. NeuroImage 23 (Suppl. 1), S208–S219.

Snider, R.S., Eldred, E., 1952. Cerebrocerebellar relationships in the monkey. J. Neurophysiol. 15, 27–40.

Sokolov, A.A., Erb, M., Gharabaghi, A., Grodd, W., Tatagiba, M.S., Pavlova, M.A., 2012. Biological motion processing: the left cerebellum communicates with the right superior temporal sulcus. NeuroImage 59, 2824–2830.

Sommer, M.A., 2003. The role of the thalamus in motor control. Curr. Opin. Neurobiol. 13, 663–670.

Stark, D.E., Margulies, D.S., Shehzad, Z.E., Reiss, P., Kelly, A.M., Uddin, L.Q., Gee, D.G., Roy, A.K., Banich, M.T., Castellanos, F.X., Milham, M.P., 2008. Regional variation in interhemispheric coordination of intrinsic hemodynamic fluctuations. J. Neurosci. 28, 13754–13764.

Stein, J.F., Glickstein, M., 1992. Role of the cerebellum in visual guidance of movement. Physiol. Rev. 72, 967–1017.

Stoodley, C.J., Schmahmann, J.D., 2009. Functional topography in the human cerebellum: a meta-analysis of neuroimaging studies. NeuroImage 44, 489–501.

Stoodley, C.J., Schmahmann, J.D., 2010. Evidence for topographic organization in the cerebellum of motor control versus cognitive and affective processing. Cortex 46, 831–844.

Stoodley, C.J., Stein, J.F., 2013. Cerebellar function in developmental dyslexia. Cerebellum 12, 267–276.

Stoodley, C.J., Valera, E.M., Schmahmann, J.D., 2012. Functional topography of the cerebellum for motor and cognitive tasks: an fMRI study. NeuroImage 59, 1560–1570.

Sultan, F., 2002. Brain evolution — analysis of mammalian brain architecture. Nature 415, 133–134.

Sultan, F., Glickstein, M., 2007. The cerebellum: comparative and animal studies. Cerebellum 6, 168–176.

Sundermann, B., Pfleiderer, B., 2012. Functional connectivity profile of the human inferior frontal junction: involvement in a cognitive control network. BMC Neurosci. 13, 119.

Thach, W.T., 1997. Context-response linkage. Int. Rev. Neurobiol. 41, 599–611.

Thach, W.T., 1998. A role for the cerebellum in learning movement coordination. Neurobiol. Learn. Mem. 70, 177–188.

Thickbroom, G.W., Byrnes, M.L., Mastaglia, F.L., 2003. Dual representation of the hand in the cerebellum: activation with voluntary and passive finger movement. NeuroImage 18, 670–674.

Tong, Y., Lindsey, K.P., de, B.F.B., 2011. Partitioning of physiological noise signals in the brain with concurrent near-infrared spectroscopy and fMRI. J. Cereb. Blood Flow Metab. 31, 2352–2362.

Van Essen, D.C., Drury, H.A., Dickson, J., Harwell, J., Hanlon, D., Anderson, C.H., 2001. An integrated software suite for surface-based analyses of cerebral cortex. J. Am. Med. Inform. Assoc. 8, 443–459.

Vilensky, J.A., van Hoesen, G.W., 1981. Corticopontine projections from the cingulate cortex in the rhesus monkey. Brain Res. 205, 391–395.

Wang, D., Buckner, R.L., Liu, H., 2013. Cerebellar asymmetry and its relation to cerebral asymmetry estimated by intrinsic functional connectivity. J. Neurophysiol. 109, 46–57.

Wiestler, T., McGonigle, D.J., Diedrichsen, J., 2011. Integration of sensory and motor representations of single fingers in the human cerebellum. J. Neurophysiol. 105, 3042–3053.

Overlapping and Parallel Cerebello-Cerebral Networks Contributing to Sensorimotor Control: An intrinsic functional connectivity study
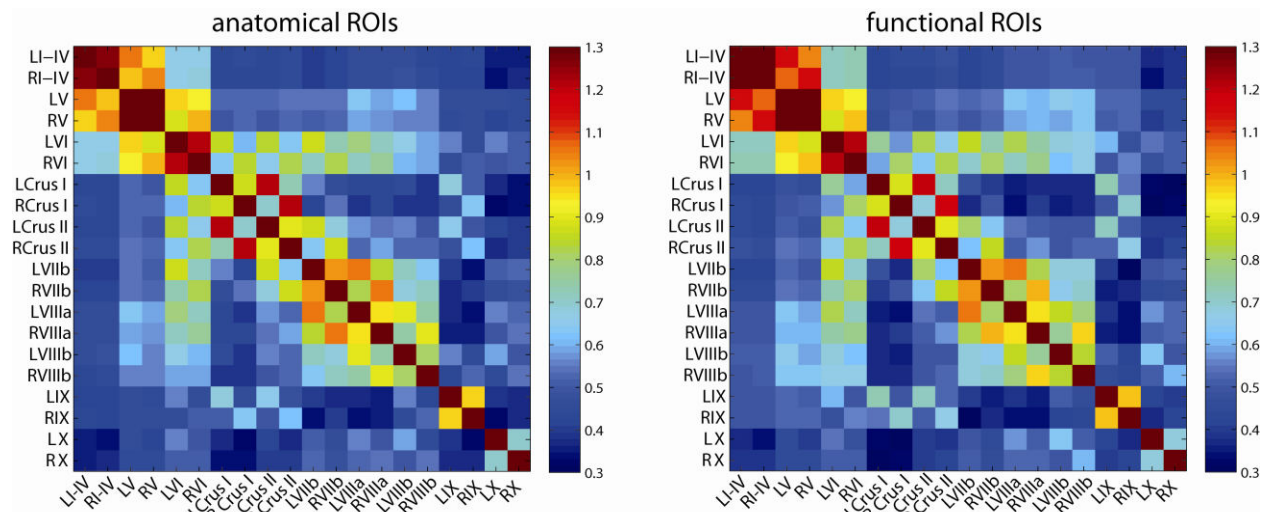

Supplementary Figure 1. Intracerebellar *r*-to-*z* transformed values, which were used to weight contrasts in the one-way ANOVA using fROIs.

Signal-Noise-Ratio analysis

SNR maps were calculated based on motion corrected functional images. Mean of voxel intensity across time was divided by the standard deviation across time. Individual SNR maps were averaged across all subjects after transformation into the SUIT space. SNR values were averaged within every aROI and fROI (Supplementary Figure 2). The mean signal-to-noise (SNR) maps of the cerebellar fROI and aROI indicate an increase in SNR after cerebello-cerebral signal separation.
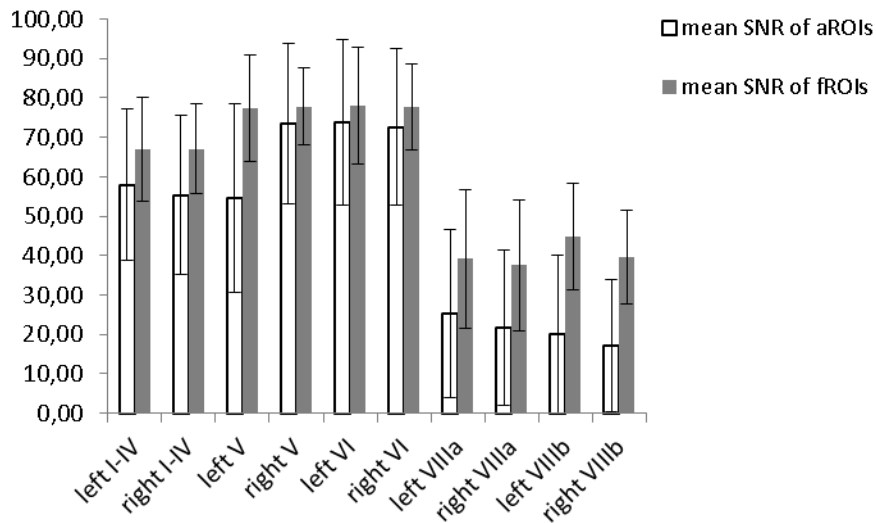
Figure 2. SNR values within the five lobules in each hemisphere (aROIs and fROIs) indicate an increase of mean SNR and decrease in standard deviation (as indicated by the error bars) when using fROIs.

Assessing iFC patterns with fROIs and aROIs

For the sake of completeness, we present the unthresholded contrast images in Supplementary Figure 3 in addition to the thresholded weighted-ANOVA results of fROIs (Fig. 3 in the main manuscript). In order to look for the quantitative differences in cerebello-thalamo-cerebral iFC patterns using aROIS and fROIS, a 2-way ANOVA was conducted including all twenty aROIs and twenty fROIs. Supplementary Figure 4 shows the main contrast fROIs>aROIs. Blue colors indicate an overall decrease of iFC by using fROIs, red colors indicate the increase in iFC.
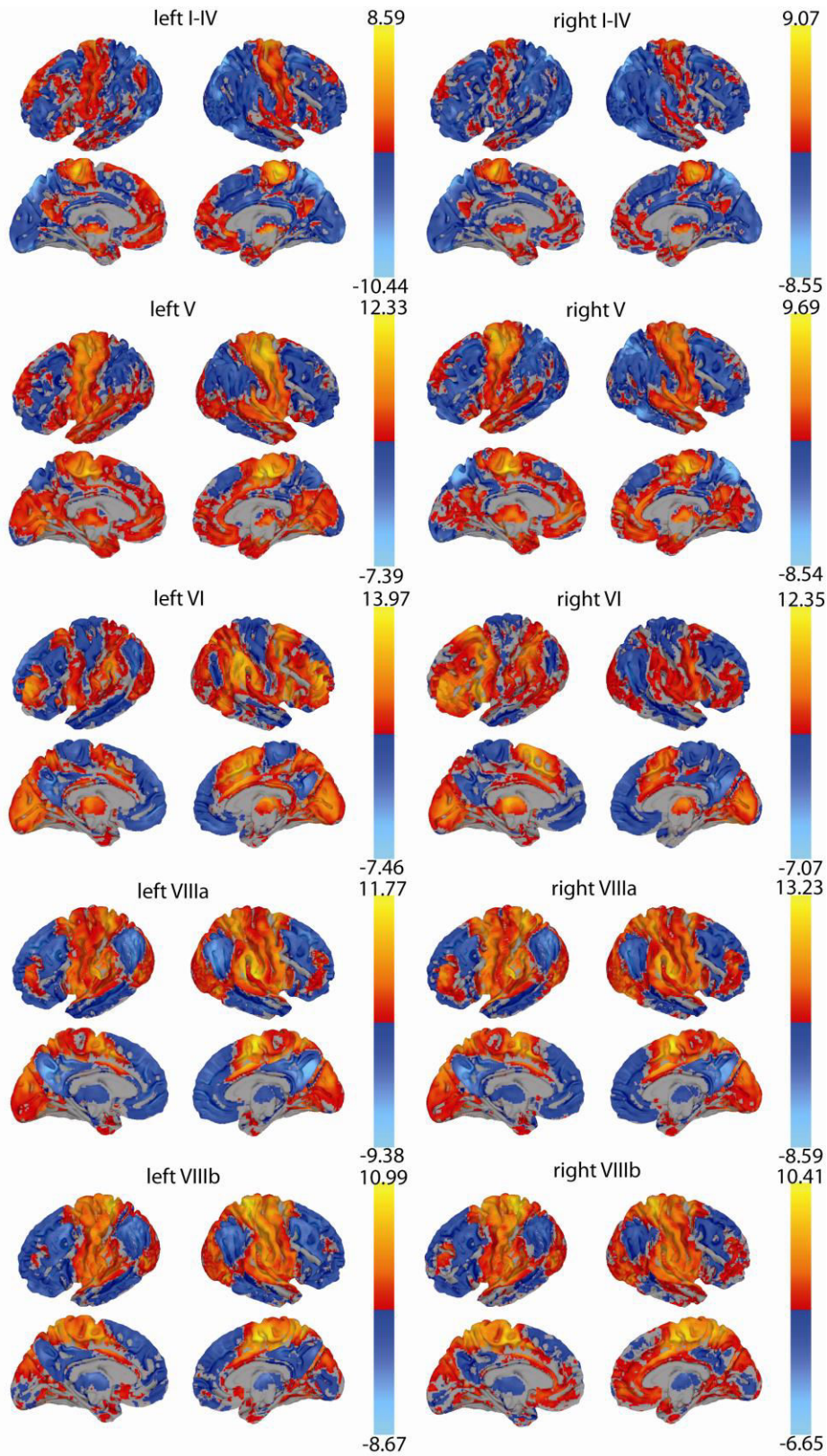
Supplementary Figure 3. Unthresholded contrast images resulting from a weighted-ANOVA with fROIs overlaid on partially inflated cortical surface maps. Color bars indicate the *t*-values.
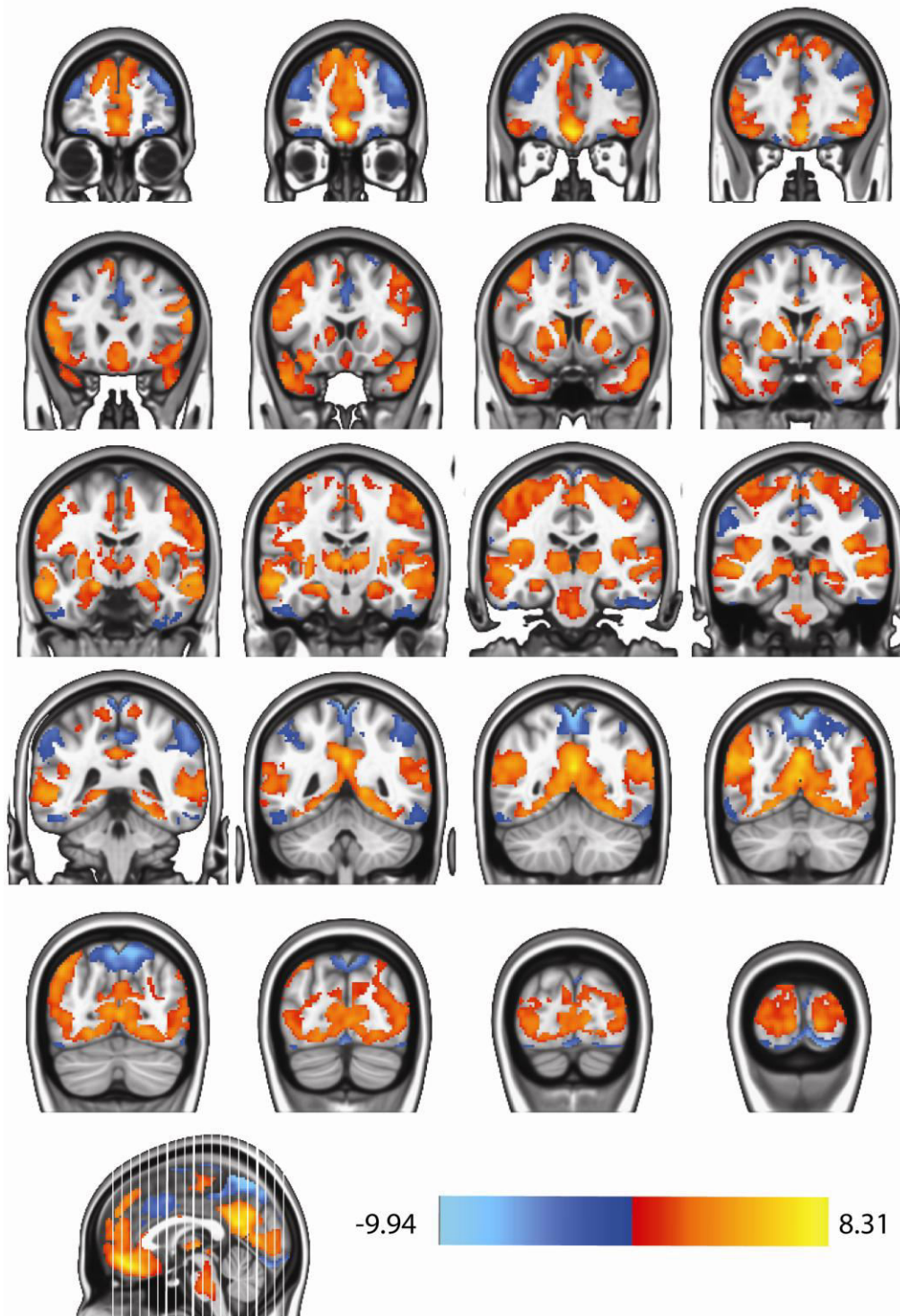
Supplementary Figure 4. Contrast of fROIs over aROIS shown as overlays on slices of a canonical anatomical image. Blue colors indicate a decrease in iFC, red colors an increase using fROIs (T=2.02, p < 0.05, FDR corrected using a cluster threshold of 148 voxels at p < 0.05 as defined by Monte-Carlo simulation). Left side shows left hemisphere.

right lobules	SM	MFG	IFG	CC	OTC	PC	OCC	PM
SM	x							
SM, OTC, PC	x					x		
	x				x			
	x				x	x		
SM, CC	x			x				
	x			x		x		
	x			x	x			
SM, IFG	x		x					
	x		x			x		
	x		x		x			
	x		x		x	x		
	x	x	x					
	x	x	x			x		
	x	x	x		x			
SM, MFG	x	x						
	x	x			x			
IFG			x					
			x			x		
			x		x			
			x	x				
PC						x		
CC				x				
OTC					x			
OTC, PC					x	x		
MFG		x						
MFG, PC		x				x		
MFG, OTC		x			x			
MFG, ACC		x		x				

left lobules	SM	MFG	IFG	CC	OTC	PC
SM	x					
SM, OTC, PC	x					x
	x				x	
	x				x	x
SM, CC	x			x		
	x			x		x
PC						x
CC				x		
CC, PC				x		x
OTC					x	
OTC, PC					x	x
MFG		x				
MFG,CC		x		x		

Supplementary Table 1. Columns show the cerebral clusters derived from the initial cerebello-cerebral partial correlation analysis. Regions in OTC, CC, PM, and OCC have been grouped together, as they were overlapping across the iFC maps of different cerebellar lobules. Rows with the same color group together combinations of cerebral clusters as displayed in Figure 4B. Crosses indicate the regions that were connected to a cerebellar voxel at a threshold of p < 0.00001, voxelwise FDR corrected.

IFG, inferior frontal gyrus; MFG, middle frontal gyrus; mPFC/CC, medial prefrontal cortex/cingulate cortex; OCC, occipital cortex; OTC, occipito-temporal gyrus; PM, premotor cortex; PC, parietal cortex; SM, sensorimotor cortex.
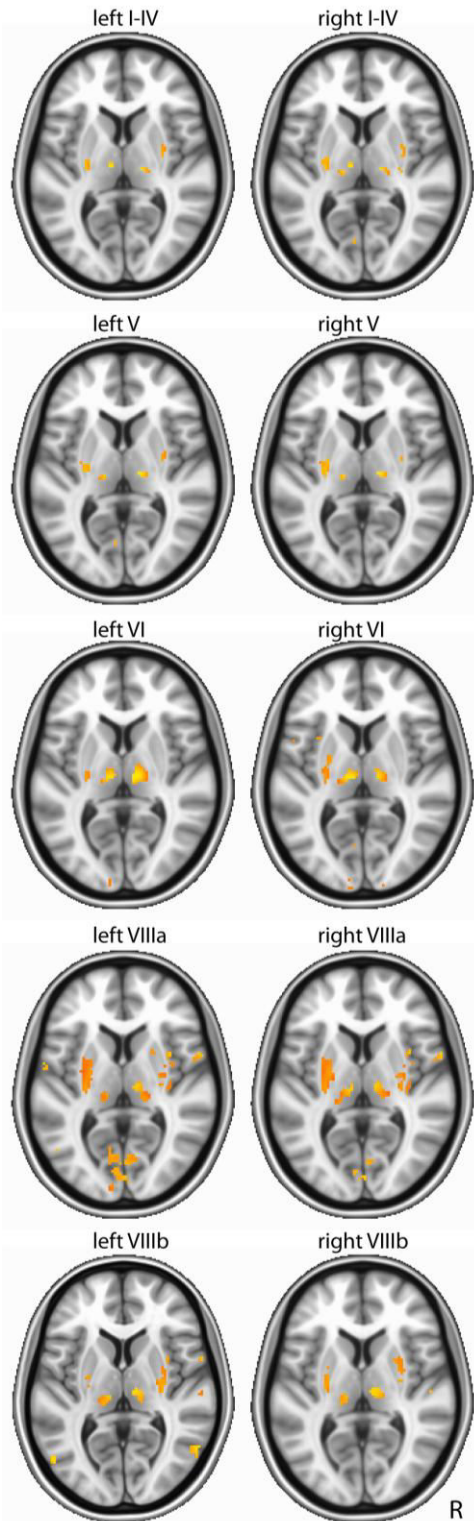
Supplementary Figure 5. Slices (y = -78) display the thalamic connectivity of the corresponding cerebellar lobules as revealed by main effects of the ANOVA. All lobular iFC maps were thresholded individually: left I-IV ($p = 2^{-15}$), right I-IV ($p = 7^{-16}$), left V ($p = 2^{-17}$), right V ($p = 6^{-18}$), left VI ($p = 5^{-18}$), right VI ($p = 2^{-18}$), left VIIIa ($p = 3^{-15}$), right VIIIa ($p = 3^{-16}$), left VIIIb ($p = 1^{-14}$), right VIIIb ($p = 6^{-15}$).

Mein Lebenslauf wird aus datenschutzrechtlichen Gründen in der elektronischen Version meiner Arbeit nicht veröffentlicht.

Publikationsliste

Gorgolewski, K. J., Lurie D., Urchs S., **Kipping, J. A.**, Craddock R. C., Milham M. P., Margulies D. S., Smallwood J. (In Review.) A correspondence between the brain's intrinsic functional architecture and the content and form of self-generated thoughts.

Schäfer A., Quinque, E. M., **Kipping, J. A.**, Arélin, K., Roggenhofer, E., Frisch, S., Villringer, A., Mueller, K., Schroeter, M. (2014). Early small vessel disease affects fronto-parietal and cerebellar hubs in close correlation with clinical symptoms – A resting-state fMRI study. Journal of Cerebral Blood Flow and Metabolism. In press.

Karim, A., Schneider, M., **Kipping, J. A.,** Kotchoubey, B., Khedr, E., Fallgatter, A., Birbaumer, N. (2013). Psychopathic traits and the psychophysiology of deception: A transcranial direct current stimulation (tDCS) study. Clinical Neurophysiology, 124(10), e57-e58.

Kipping, J. A., Grodd, W., Kumar, V., Taubert, M., Villringer, A., & Margulies, D. S. (2013). Overlapping and parallel cerebello-cerebral networks contributing to sensorimotor control: An intrinsic functional connectivity study. NeuroImage, 83: 837-848.

Sehm, B.*, **Kipping, J. A.***, Schäfer, A., Villringer, A., & Ragert, P. (2013). A comparison between uni- and bilateral tDCS effects on functional connectivity of the human motor cortex. Frontiers in Human Neuroscience, 7: 183.

Sehm, B., Schäfer, A., **Kipping, J. A.**, Margulies, D. S., Conde, V., Taubert, M., Villringer, A., & Ragert, P. (2012). Dynamic modulation of intrinsic functional connectivity by transcranial direct current stimulation. Journal of Neurophysiology, 108(12), 3253-3263.

Lengerer, S., **Kipping, J. A.**, Rommel, N., Weiss, D., Breit, S., Gasser, T., Plewnia, C., Krüger, R., & Wächter, T. (2012). Deep-brain-stimulation does not impair deglutition in Parkinson's disease. Parkinsonism & Related Disorders, 18(7), 847-853.

* equally contributing first authors

<u>Danksagung</u>